(4)

AD

TECHNICAL REPORT BRL-TR-2850

AN INFRA-RED INVESTIGATION OF HAN-BASED LIQUID PROPELLANTS

NATHAN KLEIN
KOON NG WONG

JUNE 1987

US ARMY BALLISTIC RESEARCH LABORATORY
ABERDEEN PROVING GROUND, MARYLAND

DISCLAIMER NOTICE

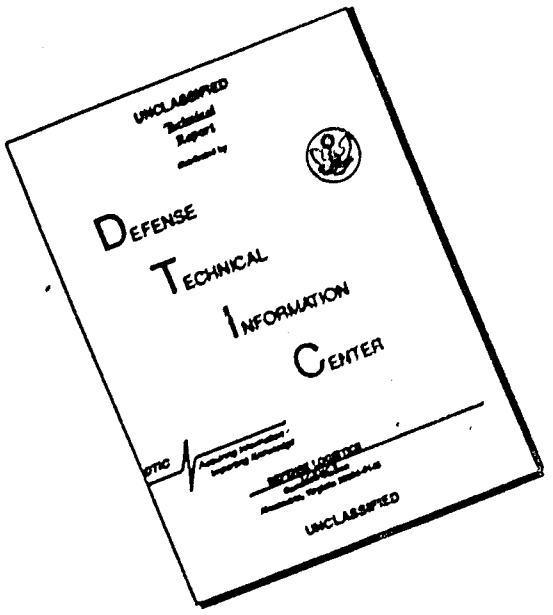

THIS DOCUMENT IS BEST QUALITY AVAILABLE. THE COPY FURNISHED TO DTIC CONTAINED A SIGNIFICANT NUMBER OF PAGES WHICH DO NOT REPRODUCE LEGIBLY.

UNCLASSIFIED
SECURITY CLASSIFICATION OF THIS PAGE

AD-A187226

REPORT DOCUMENTATION PAGE

Form Approved
OMB No 0704 0188
Exp Date Jun 30, 1986

1a REPORT SECURITY CLASSIFICATION: Unclassified	1b RESTRICTIVE MARKINGS
2a SECURITY CLASSIFICATION AUTHORITY	3 DISTRIBUTION / AVAILABILITY OF REPORT
2b DECLASSIFICATION / DOWNGRADING SCHEDULE	
4 PERFORMING ORGANIZATION REPORT NUMBER(S): BRL-TR-2850	5 MONITORING ORGANIZATION REPORT NUMBER(S)
6a NAME OF PERFORMING ORGANIZATION: US Army Ballistic Rsch Lab; 6b OFFICE SYMBOL (If applicable): SLCBR-IB	7a NAME OF MONITORING ORGANIZATION
6c ADDRESS (City, State, and ZIP Code): Aberdeen Proving Ground, MD 21005-5066	7b ADDRESS (City, State, and ZIP Code)
8a NAME OF FUNDING / SPONSORING ORGANIZATION; 8b OFFICE SYMBOL (If applicable)	9 PROCUREMENT INSTRUMENT IDENTIFICATION NUMBER
8c ADDRESS (City, State, and ZIP Code)	10 SOURCE OF FUNDING NUMBERS: PROGRAM ELEMENT NO.; PROJECT NO: D155 AB-A; TASK NO; WORK UNIT ACCESSION NO

11 TITLE (Include Security Classification)
AN INFRA-RED INVESTIGATION OF HAN-BASED LIQUID PROPELLANTS

12 PERSONAL AUTHOR(S)
Klein, Nathan, and Wong, Koon Ng

13a TYPE OF REPORT	13b TIME COVERED	14 DATE OF REPORT (Year, Month, Day)	15 PAGE COUNT
TR	FROM _____ TO _____		

16 SUPPLEMENTARY NOTATION

17 COSATI CODES		
FIELD	GROUP	SUB-GROUP

18 SUBJECT TERMS (Continue on reverse if necessary and identify by block number)
Liquid Propellants; Hydroxylammonium Nitrate; HAN; Structure; Analysis, LGP 1845, FTIR, Infrared

19 ABSTRACT (Continue on reverse if necessary and identify by block number)

This report deals with the use of Fourier transform infrared spectroscopy (FTIR) for study of the hydroxylammonium nitrate (HAN), aqueous liquid propellants. Several subjects are addressed. The feasibility of total assay of propellant, involving the simultaneous analysis of all of the components is demonstrated. A quantitative method for determination of HAN concentration that is suitable for continuous on-line use at a production facility is described. Finally, the structure of HAN-water mixtures as a function of concentration is explored in detail. HAN is highly soluble, producing homogeneous mixtures at room temperature with salt concentrations in excess of 16 mole/l. Changes in the vibrational spectra of all three components, HA^{+}, NO_3^{-}, and (H_2O), provide a consistent picture of the interactions between these species. The nitrate spectrum is most sensitive to interactions between the species present because distinctive

20 DISTRIBUTION / AVAILABILITY OF ABSTRACT	21 ABSTRACT SECURITY CLASSIFICATION
☒ UNCLASSIFIED/UNLIMITED ☐ SAME AS RPT ☐ DTIC USERS	Unclassified
22a NAME OF RESPONSIBLE INDIVIDUAL: Nathan Klein	22b TELEPHONE (Include Area Code): (301) 278-6173; 22c OFFICE SYMBOL: SLCBR-IB-B

DD FORM 1473, 84 MAR — 83 APR edition may be used until exhausted. All other editions are obsolete.

SECURITY CLASSIFICATION OF THIS PAGE
UNCLASSIFIED

19. ABSTRACT (Con't)

bands due to ion-pairing and hydration are observed. Changes in the nitrate spectrum characteristic of ion hydration are seen in dilute solution and, as concentration increases, features attributable to ion-pairs become evident and eventually dominate the spectra. The spectra of the other components provide evidence that the ion-paired species is strongly hydrogen bonded via the HA^{+} O-H group.

TABLE OF CONTENTS

LIST OF FIGURES

I. INTRODUCTION

Mixtures of hydroxylammonium nitrate (HAN), triethanolammonium nitrate (TEAN), and water, with a salt content of approximately 80 weight percent, are the liquid monopropellants that are currently being considered for use in medium-to-large caliber artillery guns. Calculated impetus of the propellants increases as the TEAN content is increased and is near its maximum value at N_2, CO_2 stoichiometry. Energy content is a function both of the HAN:TEAN ratio and the total nitrate concentration whereas thermal initiation temperature is dependent solely on nitrate concentration.[1] Although thermal initiation temperature is dependent solely on total nitrate concentration, the rate of gas production after initiation is related to the structure of the organic salt used,[2] the salts of tertiary amines producing gas at rates such that propellants consisting of HAN and a tertiary aliphatic amine nitrate are best suited for use in guns. Formulation of the propellants LGP 1845 and 1846 is based in part on these findings and the composition of the propellants is shown in Table 1.

TABLE 1. Propellant Compositions

Propellant	Composition					
	HAN		TEAN		Water	
	(wt %)	(M)	(wt %)	(M)	(wt %)	(M)
1845	63.23	9.62	19.96	1.38	16.81	13.64
1846	60.79	9.09	19.19	1.30	20.02	15.93

The propellants are compounded with a HAN:TEAN molar ratio of 7 thus providing the stoichiometry mentioned above, LGP 1846 having a somewhat lower impetus than LGP 1845 (936 J/g versus 972 J/g) because of its higher water content.

Since both HAN and TEAN are nitrates, the propellants consist of two cations and a common anion. These mixtures are homogeneous liquids that are colorless and odorless, are electrically conducting, and exhibit a vapor pressure that is lower than the partial pressure of the water present. These

properties are, to a large extent, expected since the propellants are mixtures of simple ionic salts although salt concentration is high enough that they have properties characteristic of molten salts. The mixtures remain homogeneous when cooled, eventually forming glasses at temperatures well below -50°C.[3] Although many of the physical properties of the propellants and of concentrated HAN-water mixtures support the proposition that these materials are low-temperature molten salts,[4] little information is available as yet that describes the structure and organization of the melt on a microscopic scale. Such information is needed in order to develop accurate models of the system, capable of predicting physical properties and reaction pathways.

Infra-red spectroscopy has long been recognized as a method for detailed study of chemical systems. The infrared region contains the vibrational modes of the functional groups in a particular molecule. These modes are usually sensitive to the chemical bonds in their immediate neighborhood, and to weak inter- and intra-molecular phenomena such as hydrogen-bonding and ion-pairing. The assembly of functional groups and the often complex effects of neighboring structures produces the richly detailed spectra characteristic of the infrared region. These spectra are often unique to a particular compound and can therefore be used for identification. The recent development of spectroscopic techniques based on use of the Fourier transform has greatly expanded experimental capabilities in this region and has made detailed and sensitive quantitative analysis readily achievable.[5]

This report deals with the use of infrared spectroscopy for study of the HAN-based liquid propellants. Several subjects are addressed. The feasibility of total assay of propellant, involving the simultaneous analysis of all of the components is demonstrated. A quantitative method for determination of HAN concentration that is suitable for continuous on-line use at a production facility is described. Finally, the structure of HAN-water mixtures as a function of concentration is explored in detail, leading to a self-consistent description of the molecular organization and structure of the system.

II. BACKGROUND

1. INFRARED SPECTROSCOPY

A Fourier Transform Infrared (FTIR) spectrometer differs fundamentally from the more conventional dispersive spectrometer in that the interferometer used in an FTIR instrument modulates polychromatic radiation in time rather than in space, and a complete spectrum is contained in each interferogram. The Fourier transform is then used to convert the time domain data to the frequency domain. The narrow slits needed to obtain resolution in a dispersive instrument are eliminated, resulting in a substantial increase in energy throughput. This, in turn, improves signal-to-noise (S/N) ratio and makes possible the accurate measurement of small signals. The high energy throughput and speed that are characteristic of an FTIR instrument permit a spectral scan to be acquired in seconds; multiple scans at high resolution can be acquired in reasonable times. On the assumption that noise in the data is random, multiple scans and signal averaging reduces noise because data accumulate linearly whereas noise accumulates as the square root of the number of scans. Thus, noise is reduced rapidly and the precision with which either small signals, or small differences in large signals, can be determined increases accordingly. The accurate measurement of both weakly absorbing spectral bands and small differences in bands that result from small concentration differences in the samples being studied is the ultimate benefit derived from increased sensitivity. Since the resolving power of an FTIR spectrometer is a function of the path difference between the two light beams that produce the interferogram, resolution and sensitivity are not coupled as they are in a dispersive spectrometer, and weakly absorbing spectral features can be measured without sacrificing the resolution of the system. In addition, the richness of detail commonly observed in high resolution spectra further enhances the possibility of detecting spectral differences.

Attenuated total reflectance (ATR) is a sample-handling method for obtaining the spectra of non-transparent materials. It is based on the absorption of radiation by the sample when it is in intimate contact with a crystal of high refractive index.[6] The radiation is transmitted in the crystal and is focussed at the surface at an angle of incidence greater than

the critical angle. Depth of penetration of the beam into the sample is dependent on the frequency of the incident radiation, the refractive indices of the crystal and the sample, and the angle of incidence. Although the Beer-Lambert Law cannot be applied because sample thickness is rarely known, absorbance is often observed to vary linearly with concentration and quantitative data are obtainable. The cylindrical internal reflectance (CIRcle) cell is a type of ATR accessory especially well suited for obtaining the FTIR spectra of liquids, especially aqueous samples. The theoretical basis for these methods has been developed[7] and convenient, micro-volume cells are commercially available. The optical diagram of a CIRcle cell is shown in Figure 1.

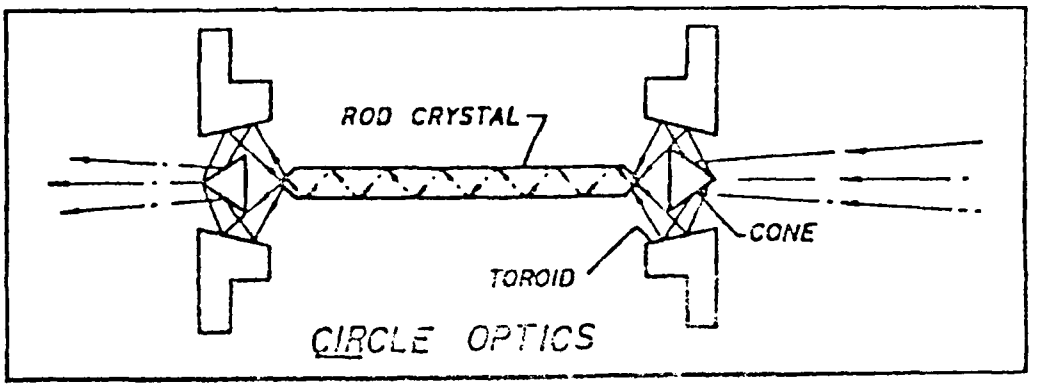

Figure 1. Optical Diagram of a Cylindrical Internal Reflectance (CIRcle) Sample Cell

2. ANALYTICAL REQUIREMENTS

It is expected that HAN will be produced in quantity by the electrolytic reduction of nitric acid.[8] Although production technology does not yet exist for this material, it is anticipated that a modern production facility will be developed and that analysis for quality control purposes will be automated and fully integrated. An on-line, continuous, analytical method for both HAN purity and composition is therefore required.

HAN, $NH_3OH^+NO_3^-$, is an inorganic salt with a melting point of 48°C and is sufficiently miscible with water that a 95 wt % HAN mixture is a homogeneous liquid at room temperature. This property allows HAN, unlike most other nitrate salts, to be studied as a liquid at very high concentrations while at room temperature. The ability to vary the HAN:water ratio over a very wide range presents an opportunity for experimentally observing the transition from dilute solution to salt melt, and the effect of such transition on the organization of the ions and solvent.

TEAN, $[(HOCH_2CH_2)_3NH]^+NO_3^-$, the third component of the propellants, is a white, crystalline, salt that is hygroscopic and readily soluble in water. It has a melting point of 80.4°C[9] and forms aqueous solutions that saturate at concentrations slightly below 5 M at room temperature. It thus exhibits the concentrative properties of a conventional ionic salt, and it would be expected that its solutions possess the properties of conventional aqueous solutions.

FTIR spectroscopy shows promise for simultaneous determination of all of the major propellant components.[10 11] It is important to bear in mind that spectral bands chosen for quantitative analytical use should not be especially sensitive to changes in solution structure or molecular organization, but should respond in a direct and simple manner to changes in component concentration. Thus, the spectral bands most useful for structure elucidation are often the worst bands to consider for quantitative analysis.

3. VIBRATIONAL SPECTRA OF HAN

The infrared spectra at low temperature of the halide salts of hydroxylamine have been recorded and analysed,[12] as have the spectra at room temperature of these compounds, their deuterated homologs, and the nitrate, sulfate, and perchlorate salts.[13] The Raman spectrum of aqueous 11 M HAN was recorded and analyzed by Van Dijk and Priest.[14] Cronin and Brill[15] studied the FTIR spectrum of solid HAN from 170 K to temperatures at which decomposition takes place. Fifer has reported[16] the FTIR spectra of concentrated aqueous and deuterated HAN solutions at different temperatures. His band assignment for the O-H stretching mode of the hydroxylammonium ion, HA^+,

differed significantly from values previously reported.[12-14] He concluded, using the Novak correlation,[17] that the O--O bond distance in the O-H--O hydrogen bond with NO_3^- in the liquid was 2.61 Å, independent of both temperature and concentration. Cronin and Brill[15] also determined the crystal structure of HAN and showed that HA^+ is surrounded by four nitrate ions. All four of the HA^+ protons can form hydrogen bonds with the oxygen atoms of NO_3^- and the O--O distance in the O-H--O hydrogen bond is 2.80 Å. They suggested that Fifer's O-H assignment was erroneous and that the Novak correlation was not valid in this case.

Vanderhoff and Bunte[18] attempted to elucidate the structure of aqueous HAN solutions using the vibrational spectrum of the nitrate ion. They studied the laser Raman spectra of 3, 7, and 13 M aqueous HAN in the $\nu_4(E')$ and $\nu_1(A_1')$ regions. Since the ν_4 band, considered a good diagnostic for contact ion-pairing,[19] did not show any splitting, even at 13 M, they concluded that there was no evidence for substantial contact ion-pairing in aqueous HAN. They did notice that the ν_4 band shifts to lower frequencies as concentration decreases and, that at 13 M the band is asymmetrical.

Detailed HAN-water spectral data can resolve issues still pending, provide the basis for quantitative analysis, and produce additional and unequivocal evidence concerning the structure of these mixtures. Since such evidence will be derived from infrared vibrational measurements that relate closely to fundamental structural properties, they will complement physical property data already available and either reinforce or negate conclusions based on such property data.

III. EXPERIMENTAL METHODS AND RESULTS

Infrared spectra were recorded using a Mattson* Sirius 100 FTIR spectrometer equipped with a liquid nitrogen cooled mercury cadmium telluride (MCT) detector. Samples were contained in a Barnes** micro cylindrical-

---

*Mattson Instruments, Inc, Madison, WI.

** Barnes Analytical Div., Spectra-Tech, Inc., Stamford, CT.

internal-reflection (CIRcle) cell containing a zinc selenide rod. Sample volume of the cell is approximately 25 μ liter. The spectrometer was continuously purged with argon in order to minimize interferences from carbon dioxide and water vapor. Samples were introduced via a small pump located just outside the spectrometer. The samples were flushed through the cell until an unvarying spectrum was obtained before data were recorded. Background was a single beam spectrum of the empty cell filled with Ar gas. All spectra were recorded at 4 cm^{-1} resolution and are the result of co-addition of between 100 and 500 scans.

HAN was prepared from Reagent Grade, 2.8 M solution (Southwest Analytical Chemicals) by water stripping at 40°C under vacuum. A mixture in excess of 94 wt % was prepared and diluted with distilled water to provide samples covering the concentration range 0.01-16 M. The HAN and water concentrations of the samples used are listed in Table 2.

TABLE 2. Composition of Aqueous HAN Mixtures

HAN (M)	Water (M)	Water:HAN Molar Ratio
16	8	0.5
14	14	1
12	22	1.8
10	26	2.6
8	32	4
4	45	11
2	52	26
1	55	55
0.8	55	69
0.4	55	138
0.2	55	275
0.1	55	550
0.08	55	688
0.04	55	1375
0.02	55	2750
0.01	55	5500

The infrared spectrum of aqueous HAN is complex, containing contributions from the HA^+ and NO_3^- ions and from the water molecule. In order to simplify data interpretation, the spectra of aqueous hydroxylammonium chloride (HAC) and of water-tetrahydrofuran (THF) mixtures were also recorded. Analytical Grade HAC (Mallinkrodt Chemical Works) was used without further purification. HAC is not as soluble in water as HAN, 8 M being the highest

concentration obtainable at room temperature. FTIR spectra of 8, 6, 4, 2, and 1 M HAC solutions were recorded. Water spectra over the concentration range 0.1-55 M were obtained on water-THF mixtures. THF was chosen as the solvent because its spectral absorption bands barely overlap those of water.

TEAN was obtained as a crystalline solid from the Elkton Division of Morton-Thiokol, Inc. and was used without further purification. LGP 1845 was obtained from the same source. TEAN solutions were prepared with distilled water; the maximum TEAN concentration used was 4.81 M, which is close to saturation at room temperature.

Spectra of the separate propellant components were obtained as a function of concentration. Water-THF spectra are shown in Figure 2. Although spectra were obtained over the water concentration range 55.5-0.1 Molar, for purposes of clarity, only the 55, 40, 20, 10, and 4 M spectra are shown in Figure 2.

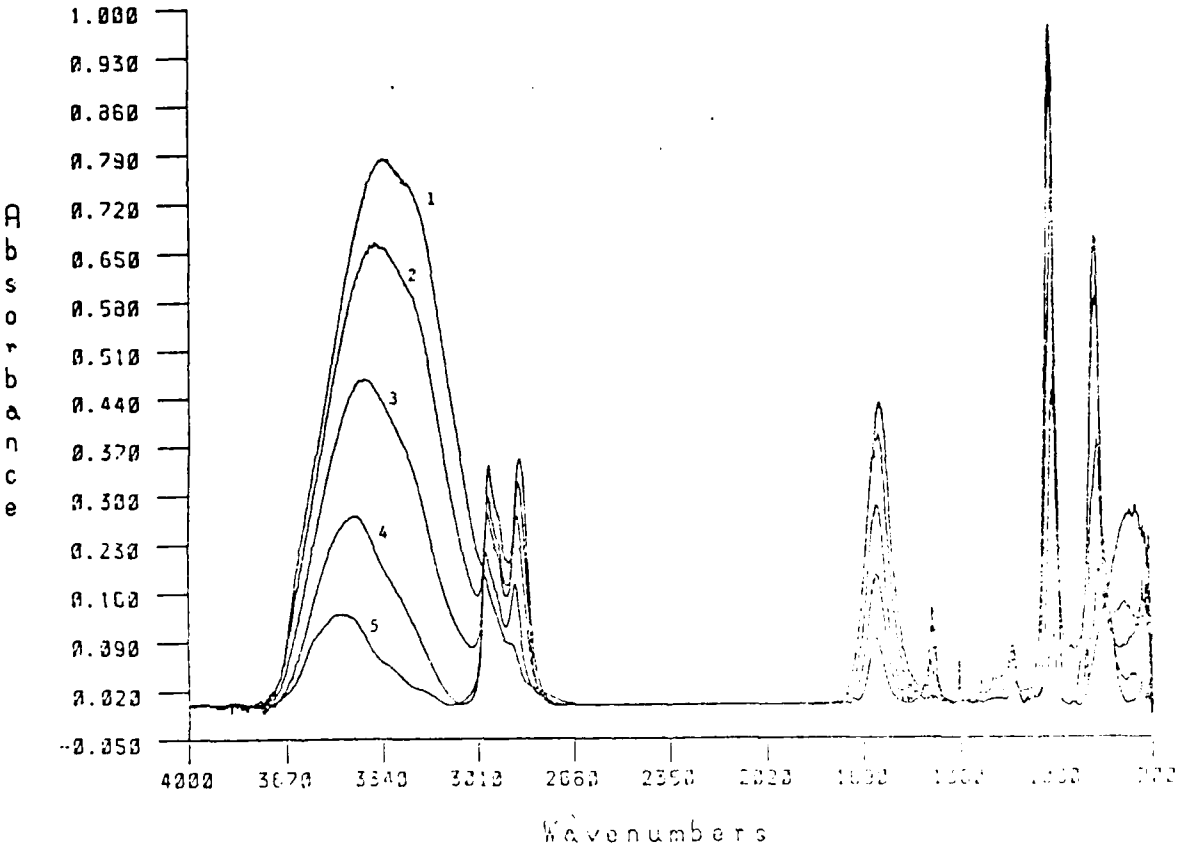

Figure 2. FTIR Spectra of Water-THF Mixtures: 1 = 55M, 2 = 40M, 3 = 20M, 4 = 10M, 5 = 4M

The spectra of HAN-water mixtures are shown in Figures 3 and 4. Figure 3 covers the spectral region 700-4000 cm^{-1} and is limited to HAN concentrations of 1, 2, 4, 10, and 14 Molar. A portion of the Figure 3 data covering only the spectral region 900-1600 cm^{-1} is shown in Figure 4. Additional spectra obtained from 8, 12, and 16 Molar HAN are included in Figure 4. In both Figures the spectra show complex, concentration dependent features.

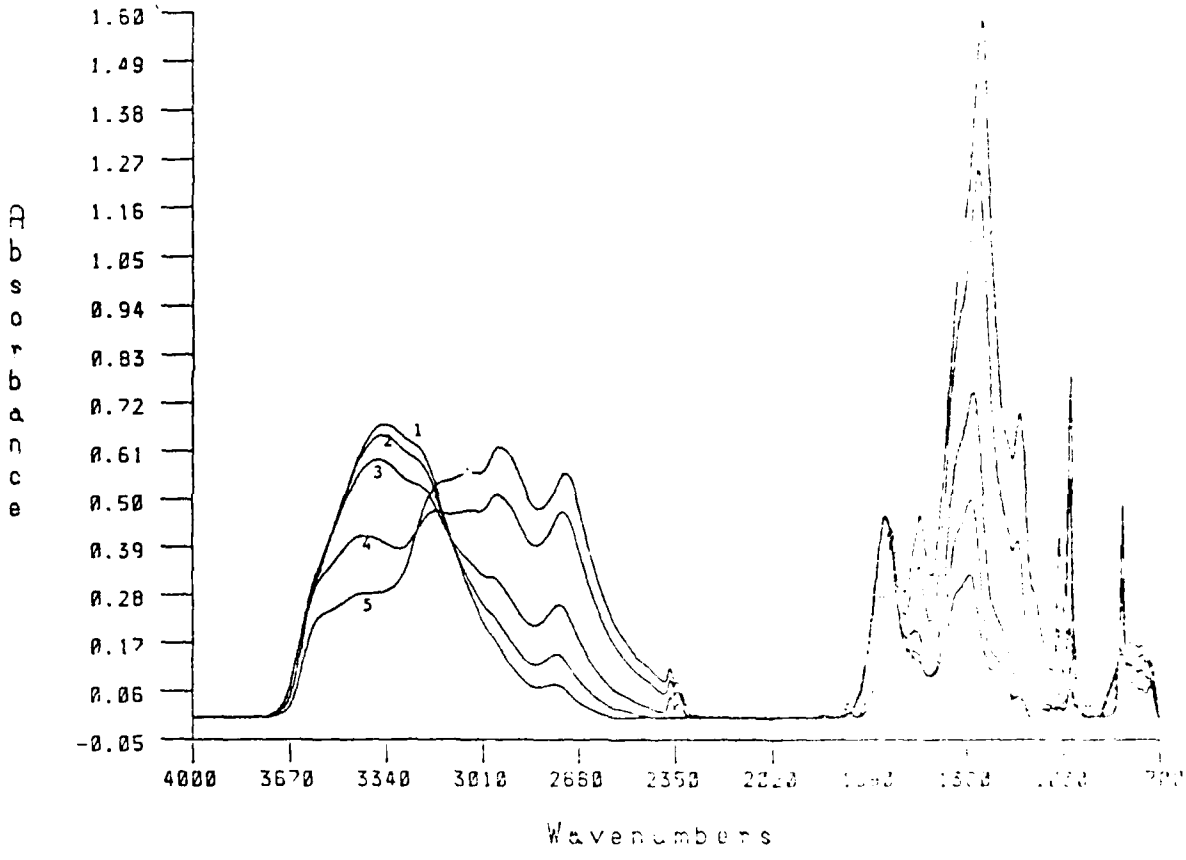

Figure 3. FTIR Spectra of HAN-Water Mixtures: 1 = 1M, 2 = 2M, 3 = 4M, 4 = 10M, 5 = 14M

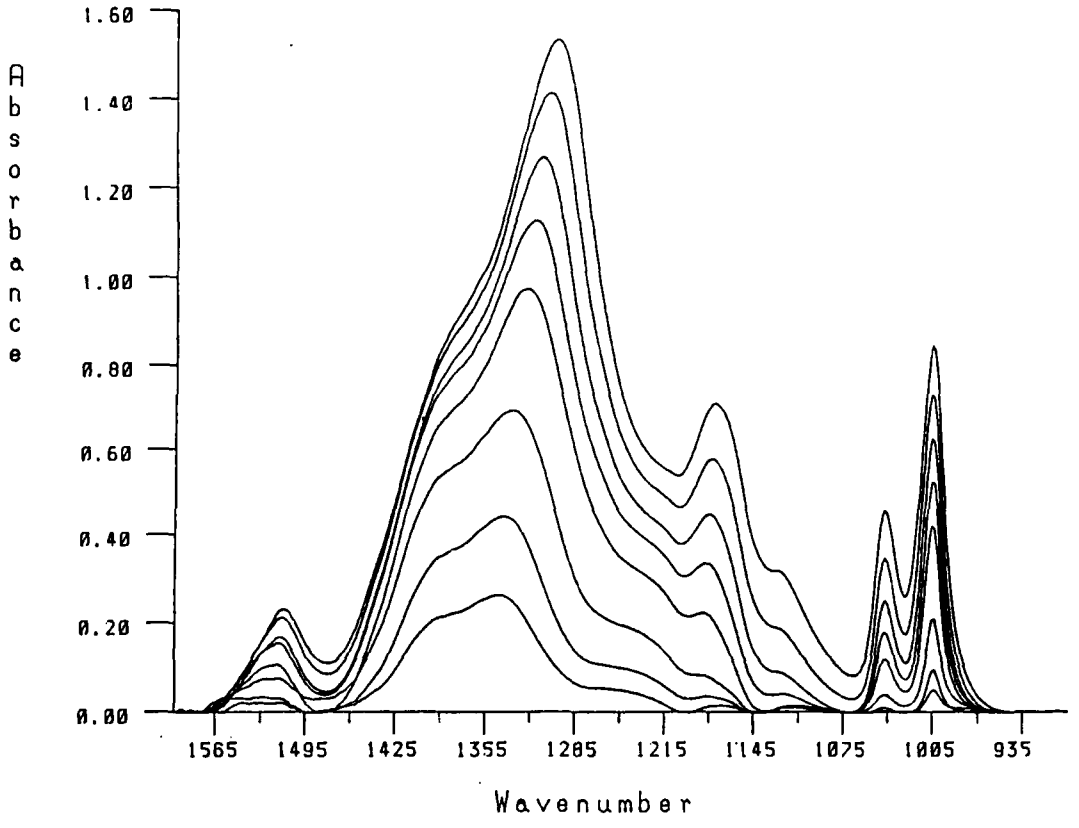

Figure 4. Aqueous HAN: Spectral Range = 900-1600 cm^{-1}, HAN Concentration = 1, 2, 4, 8, 10, 12, 14, 16 Molar

TEAN-water spectra, obtained as a function of concentration, are shown in Figure 5.

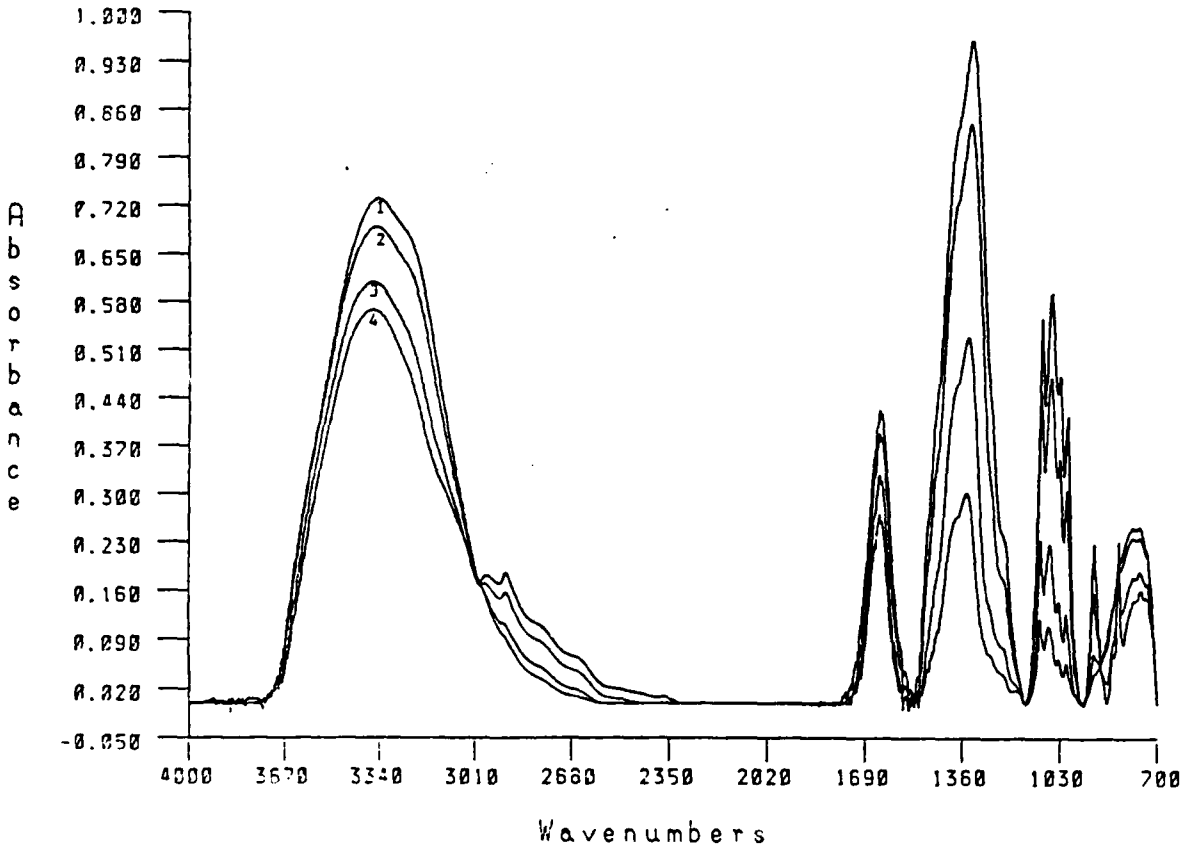

Figure 5. FTIR Spectra of TEAN-Water Mixtures: 1 = 4.81M, 2 = 4M, 3 = 2M, 4 = 1M

The FTIR spectrum of LGP 1845 is presented in Figure 6. As noted in Table 1, this mixture is 9.62 M in HAN, 1.38 M in TEAN, and 13.64 M in water. A synthetic spectrum created by combining the spectra at appropriate concentrations of the individual components of the propellant is included for comparison.

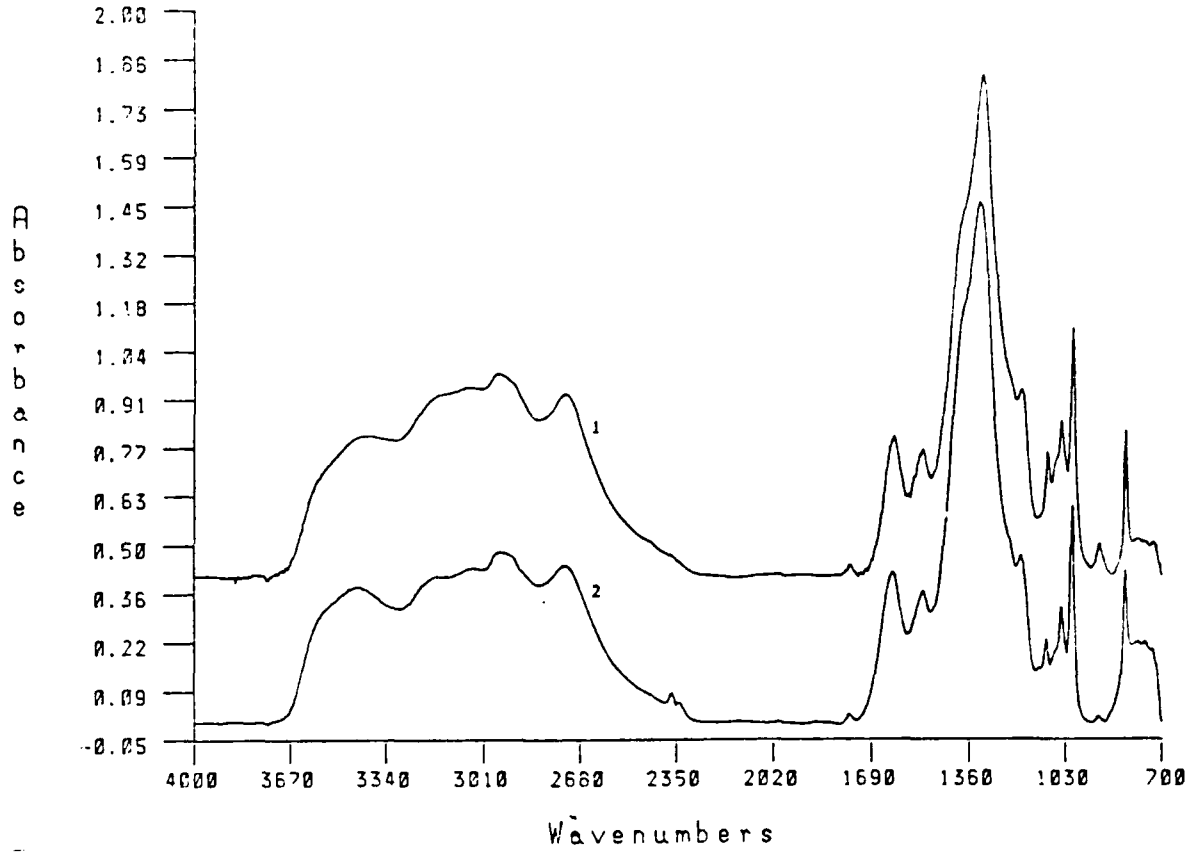

Figure 6. FTIR Spectrum of LGP 1845: 1 = LGP1845, 2 = Synthetic Spectrum

IV. DISCUSSION

1. THE SPECTRA AND STRUCTURE OF HAN-WATER MIXTURES

The concentrative properties of the HAN-water system together with the FTIR-CIR technique permits acquisition and evaluation of spectra over a very wide concentration range. The three components, HA^+, NO_3^-, and H_2O, each has a distinct, and to a large extent, non-overlapping vibrational spectrum.

Although the spectrum of the nitrate ion alone is extremely sensitive to changes in its environment and has been extensively used as a structure probe[19 20] to provide evidence for ion-pairing and hydration, the spectra of the cation and solvent should provide additional information about these interactions.

a. The FTIR spectrum of the nitrate ion. The isolated NO_3^- ion has D_{3h} symmetry with six normal vibrations, they are $\nu_1(A_1')$, Raman active only; $\nu_2(A_2")$, infrared active only; $\nu_3(E')$, Raman and infrared active; $\nu_4(E')$, Raman and infrared active. The ν_3 and ν_4 modes are doubly degenerate, so the vibrational spectrum of the isolated ion should consist of four bands. It has been known for some time[21-25] that the nitrate ion interacts both with solvent and, at sufficiently high concentration, with the cation present. These interactions can destroy the symmetry of the isolated ion and remove the degeneracy of ν_3 and ν_4 . The degenerate ν_3 mode is split into two bands in aqueous nitrate solutions. Although the $\nu_4(E')$ mode remains degenerate in dilute aqueous solution,[19] another band appears in the ν_4 spectral region in concentrated nitrate. This new band is believed to be caused by a new species, a contact ion-pair, and is thus not an indication of removal of the ν_4 degeneracy. The nondegenerate modes, ν_1 and ν_2 give rise, in principle, to two bands. The broadness of the bands obtained often causes lines to be hidden under a contour so that not all of the theoretically predicted bands are observed and complete resolution of the band system is rare. Observation and analysis of the band system can deteriorate to detection of an asymmetry or, if the band appears to be symmetrical, to minor changes in the overall band profile.[19 26 27] This problem could be especially severe in the case of HAN because of possible interferences from the rich vibrational spectrum of the HA^+ ion (as compared with simpler metallic nitrate systems). Fortunately, the bands of HA^+ are adequately separated from those of NO_3^- to make detailed analysis possible.

(1) The ν_3 Region (asymmetric stretch, near 1380 cm^{-1}). The ν_3 band of NO_3^- is intensely absorbing, limiting many past studies[22] to dilute solutions. The CIR technique alleviates this limitation, as seen in Figure 4, where the intense absorption between 1300 and 1430 cm^{-1} is the $\nu_3(E')$ band of the nitrate ion. Several features of this band system are noteworthy, the

most obvious of which is that ν_3 is split into two bands at all of the concentrations shown. Previous studies at low solute concentrations in hydrogen-bonding solvents[24 25] indicate that the splitting of ν_3 is caused by an asymmetrically solvated nitrate ion. The data for 0.01 M HAN locate the two ν_3 bands at 1405 and 1358 cm^{-1}, in excellent agreement with other observations.[22 24 25] As solute concentration is increased, splitting becomes dependent both on concentration and on the nature of the cation[27] causing Janz[20] to propose that $\nu_3(E')$ splitting would be a useful probe of the structure of molten salts and concentrated aqueous solutions.

Since the band near 1300 cm^{-1} shifts to lower frequency as concentration increases whereas the frequency of the band near 1400 cm^{-1} remains unchanged, splitting increases with increasing concentration. Although Figure 4 shows the 1300 cm^{-1} band to be of greater intensity than the 1400 cm^{-1} band, the 1300:1400 intensity ratio decreases with decreasing HAN concentration and an intensity reversal is observed at HAN concentrations of 0.02 M or less. It appears that the 1400 cm^{-1} band is associated with solvent interaction and it seems reasonable to assign this band to the hydrated nitrate ion. The 1300 cm^{-1} band then results from bound (ion-paired) nitrate.[21 26] At HAN concentrations above 8 M, in which water:salt ratio is less than 4 (Table 2), the growth in intensity of the 1400 cm^{-1} band with increasing HAN concentration is very small whereas the intensity of the 1300 cm^{-1} band increases at what would seem to be a normal rate. Since one could expect that the number of contact ion-pairs be significant at these high solute concentrations, assignment of the 1300 cm^{-1} band to bound nitrate is consistent with this observation. Incidentally, measurement of the electrical conductivity of HAN solutions shows[28] a maximum in specific conductance at approximately 7 M. A maximum in specific conductance usually indicates that some change has taken place in the mixture resulting in a decrease in the number of ionic species available for charge conduction or a decrease in mobility of the charge-carrying species. The conductivity data thus support the production of significant numbers of ion-pairs at HAN concentrations above 7 Molar.

Lastly, the effect of HAN concentration on the frequency of the lower frequency (near 1300 cm^{-1}) band is shown in Figure 7.

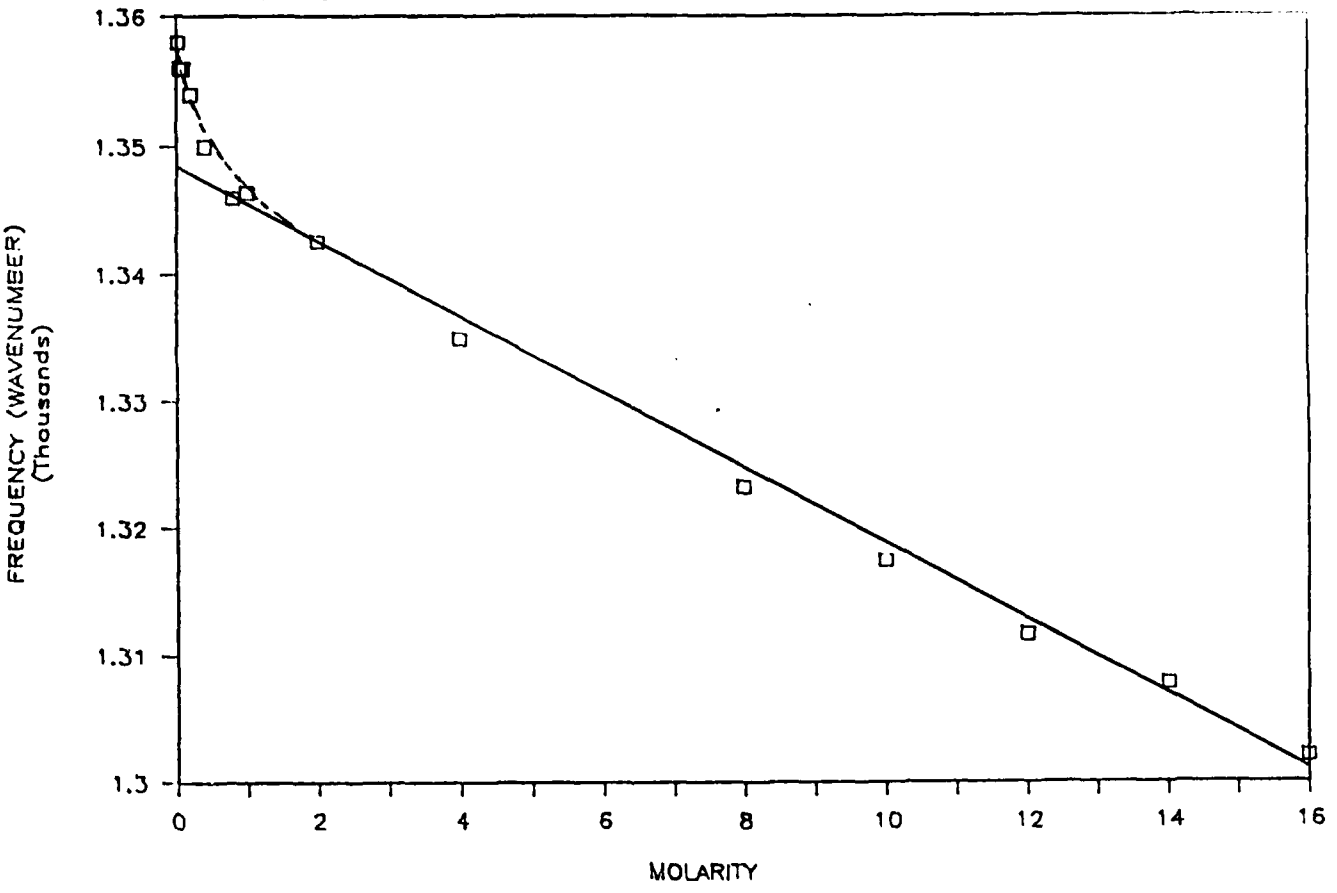

Figure 7. Effect of HAN Concentration on the Frequency of the Absorption Maximum Near 1300 cm

As mentioned previously, the frequency of this band decreases with increasing HAN concentration. A substantial change in the rate of this decrease is seen at about 0.8 M HAN and it seems reasonable to propose that ion-solvent interaction dominates at low salt concentration and that cation-anion interaction becomes significant above 0.8 M HAN. Between 0.8 and 16 M HAN, the frequency-concentration relationship appears to be linear. Since both water and salt concentrations are changing over this concentration range, the observed simple linear relationship requires that the HA^{+}-NO_3^{-} interaction be much stronger than, and thus overwhelm, the H_2O-NO_3^{-} interaction.

The preceding discussion is probably oversimplified in that it assumes only two nitrate species, the hydrated ion and the ion pair, and it further assumes that these species are essentially separate entities. The effect of cation structure on the spectrum, the existence of solvent-separated ion pairs, and several other potential interaction mechanisms are not mentioned but cannot be ruled out.

The rather simplistic argument for lifting of the mode degeneracy is also inadequate. For example, if interaction with solvent removes the ν_3 degeneracy, then interaction with cation (ion-pair formation) should also do so and four rather than two bands should be seen at intermediate nitrate concentrations. That the bands seen are in fact two bands rather than four or more bands that overlap, is not considered. The main point made in the discussion is that more than one type of interaction has been observed and that solvation and ion-pairing are plausible explanations of the data.

(2) <u>The ν_4(E') Region (bending, near 716 cm^{-1})</u>. The ν_4 band near 716 cm^{-1} is potentially a good diagnostic for nitrate ion structure because it often develops additional bands with increasing nitrate concentration. Ease of detection of the two bands is variable, however, and its use is limited. The bands are more readily resolved in solvents of lower dielectric constant; for example, the $Sr(NO_3^-)_2$-NH_3 system produces two well-defined ν_4 maxima at 723 and 709 cm^{-1}.[29] Since the frequency cut-off of the equipment used is about 650 cm^{-1} and a broad absorption caused by a water librational mode extends from 300 to 900 cm^{-1},[19] the ν_4 region is poorly suited for infrared solution structure investigations of the aqueous HAN system. Comparison of the FTIR spectra of aqueous HAC and HAN solutions show that weak features between 750 and 700 cm^{-1} are indeed produced by the nitrate ion. Baseline correction and 15-point smoothing was required to extract the data and the 16, 12, 8, and 4 M HAN spectra are shown in Figure 8. The 16 M and 4 M samples show only one band at 727 cm^{-1} and 717 cm^{-1} respectively although the lower frequency side of the 727 cm^{-1} band and the higher side of the 717 cm^{-1} band is distorted. Two bands are resolved in the 12 and 8 M samples. Strengthened by the possible observation of ion-paired and hydrated nitrate in the ν_3 region, it is reasonable to suggest that ion-pairing dominates the 16 M sample and that the 727 cm^{-1} band be assigned to ion-paired nitrate. As concen-

tration decreases, this band diminishes in favor of the lower frequency band, assigned to the hydrated ion. These data are also consistent with results obtained in a laser Raman investigation of aqueous HAN,[18] in which a ν_4 band at 727 cm^{-1} was seen in 13 M samples with a weak asymmetry on the low frequency side. Peak frequency decreases with decreasing concentration and, at 3 M, is located at about 720 cm^{-1}. Although two bands were not resolved, the lack of band resolution could be ascribed to a number of causes ranging from differences in equipment response and sensitivity to the possibility that Raman response to changes in the NO_3^- ionic environment is less than infrared response.

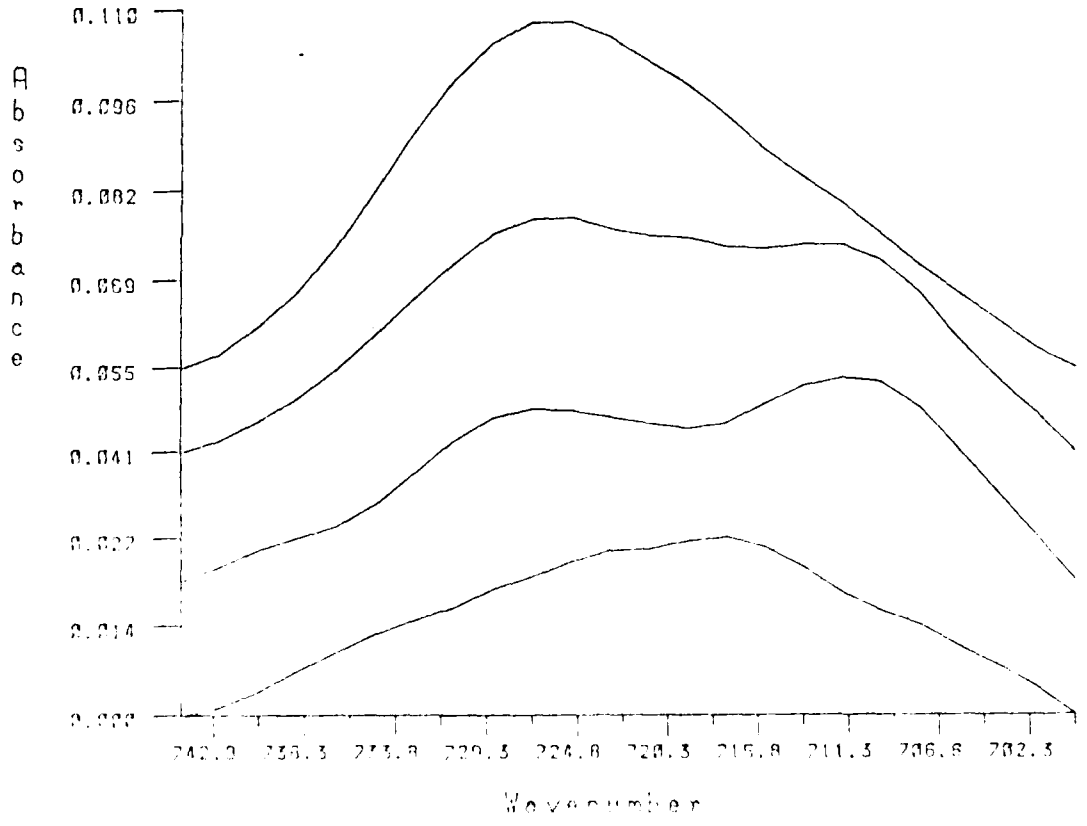

Figure 8. The Nitrate Spectrum of HAN in the ν_4 Region

(3) The $\nu_2(A_2")$ Region (bending, near 830 cm^{-1}). Resolution of the infrared active, $\nu_2(A_2")$ band near 830 cm^{-1} into two or more bands is not often reported and indeed, the FTIR-CIR spectrum of aqueous HAN in the 800 cm^{-1} region exhibits a one-band system as shown in Figure 9. The frequency of maximum absorbance shifts from 822 to 829 cm^{-1} as concentration decreases from 16 to 1 M; it is reasonable to propose that the frequency shift coincides with a shift from ion-paired to solvated nitrate.

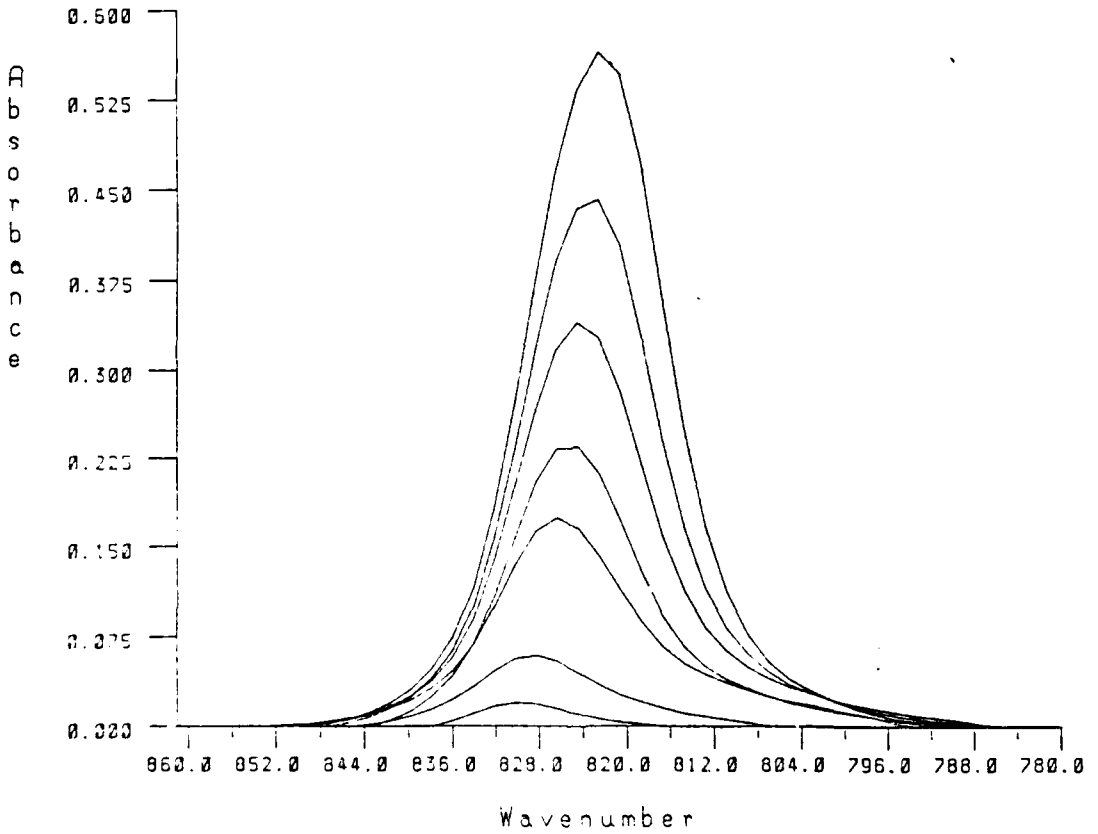

Figure 9. FTIR Spectrum of Aqueous HAN in the ν_2 Region

Figure 10 presents the area under the ν_2 band as a function of HAN concentration. As seen, area does not increase linearly and a positive curvature is observed over the entire concentration range plotted. Riddell and coworkers[27] point out that such results could indicate the presence of two or more species. The area under a symmetrical peak is proportional to peak intensity, I, which is, in turn, the product of molar absorptivity, J, and concentration, C. If total intensity, I_t, is equal to the sum of the intensities of two components, I_b and I_f, then

$$I_t = I_b + I_f = J_b C_b + J_f C_f$$

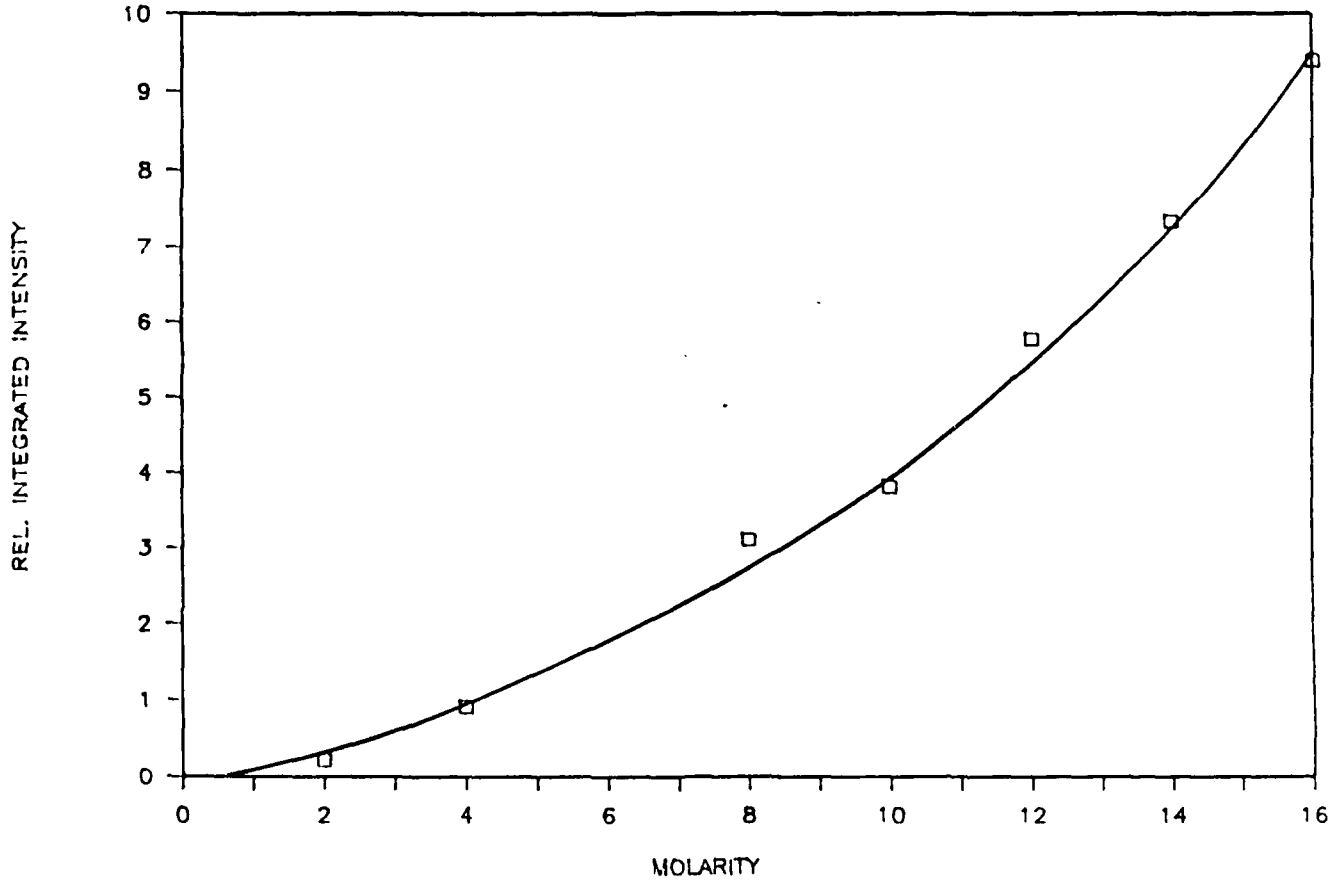

Figure 10. Area Under the ν_2 Band as a Function of HAN Concentration

where J_b and J_f are the molar absorptivities of bound (ion-paired) and free (hydrated) nitrate, and C_b and C_f are the corresponding concentrations. Total nitrate is the sum of C_b and C_f; if $J_b = J_f$, then a plot of integrated intensity vs concentration will be a straight line with an intercept of zero. Since Figure 10 shows this not to be the case, it must be assumed that $J_b \neq J_f$ which, in turn, suggests that the dipole moment is different for the two species. In fact, J_b must be larger than J_f to satisfy the Figure 10 data. The ν_2 findings thus provide further support for the proposal that two forms of nitrate exist in these HAN mixtures.

(4) The $\nu_1(A_1')$ Region (symmetric stretch, near 1050 cm^{-1}). The isolated NO_3^- ion has D_{3h} symmetry and the $\nu_1(A_1')$ symmetric stretching mode near 1050 cm^{-1} is infrared inactive. However, the band does appear in the FTIR spectrum at 1043.6 cm^{-1} (Figure 4) with an intensity almost equal to the infrared allowed $\nu_2(A_2'')$ mode, indicating that the D_{3h} symmetry has been destroyed by interaction either with solvent or with the cation. The frequency of the peak maximum remains constant over a wide concentration range. In addition, ν_1 is detected at concentrations as low as 0.2 M HAN, where cation-anion interaction is probably of minor importance. Both of these observations tend to support assignment of the 1043.6 cm^{-1} band to hydrated nitrate. However, the intensity of the ν_1 band varies with concentration in much the same manner as does the area of the ν_2 band (Figure 10), thus suggesting that similar phenomena are being observed, and that the measured intensity may be the sum of hydrated and ion-paired nitrate.

The $\nu_1:\nu_2$ intensity ratio has been used to measure degree of association[22,26] in metallic nitrate systems, a value greater than 2 being indicative of covalent bond formation. The $\nu_1:\nu_2$ ratio in aqueous HAN is approximately 0.7 and indicates that the ion-pair retains ionic character.

A summary of the nitrate data presented indicates the existence of two nitrate species in HAN-water mixtures. The dominant species is the hydrated nitrate ion at low HAN concentration. As HAN concentration is increased, a second species appears, possessing the properties expected of a nitrate-cation ion-pair. The cation is more strongly associated with nitrate than is water but retains ionic character throughout the concentration range investigated,

there being no evidence for covalent bonding at 16 M HAN, the highest concentration studied.

b. The FTIR spectrum of the HA^+ ion. Although the HA^+ and NO_3^- ions appear to form ion-pairs that profoundly affect the vibrational spectrum of the nitrate ion and indicate that the interaction is via hydrogen bonding, it does not necessarily follow that a companion effect will be seen in the HA^+ spectrum since the vibrational spectrum of the HA^+ ion might be insensitive to such interactions. A similar argument may apply to the effect of solvent on the HA^+ spectrum although HA^+-H_2O interaction via hydrogen bonding is certainly possible. Observation of the vibrational modes of the HA^+ ion thus might provide information complementary to the NO_3^- data. The HA^+ bands that are sufficiently intense and well defined to be amenable to study and are expected to interact with nitrate and/or water are the NH_3^+ degenerate rock near 1179 cm^{-1}, the NH_3^+ symmetric deformation near 1512 cm^{-1}, the combination band near 2720 cm^{-1}, the NH_3^+ symmetric stretch near 2955 cm^{-1}, and the O-H stretching mode at about 3150 cm^{-1}.[12] The portion of Figure 3 covering frequencies between 2300 and 4000 cm^{-1} is shown in greater detail in Figure 11.

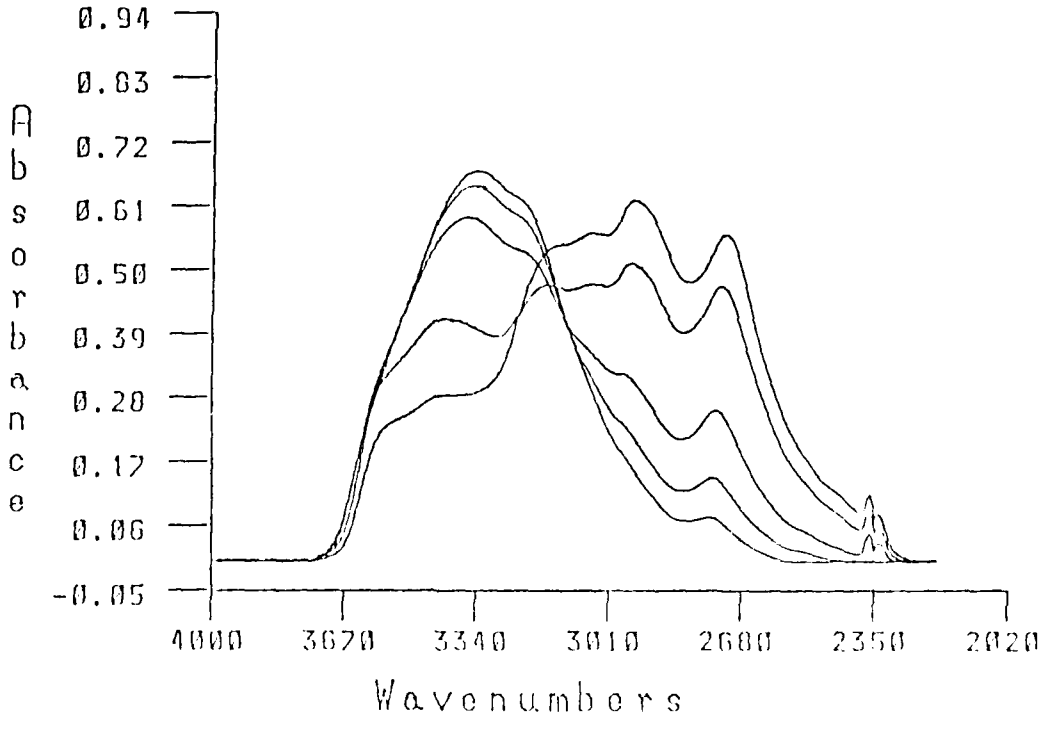

Figure 11. The Spectrum of HAN Between 2300 and 4000 cm^{-1}

As seen in Figure 11, the 2720, 2955, and 3150 cm^{-1} bands all shift to higher frequencies as HAN concentration decreases. The effect of concentration on the frequency maximum of the combination band near 2720 cm^{-1} is shown in Figure 12.

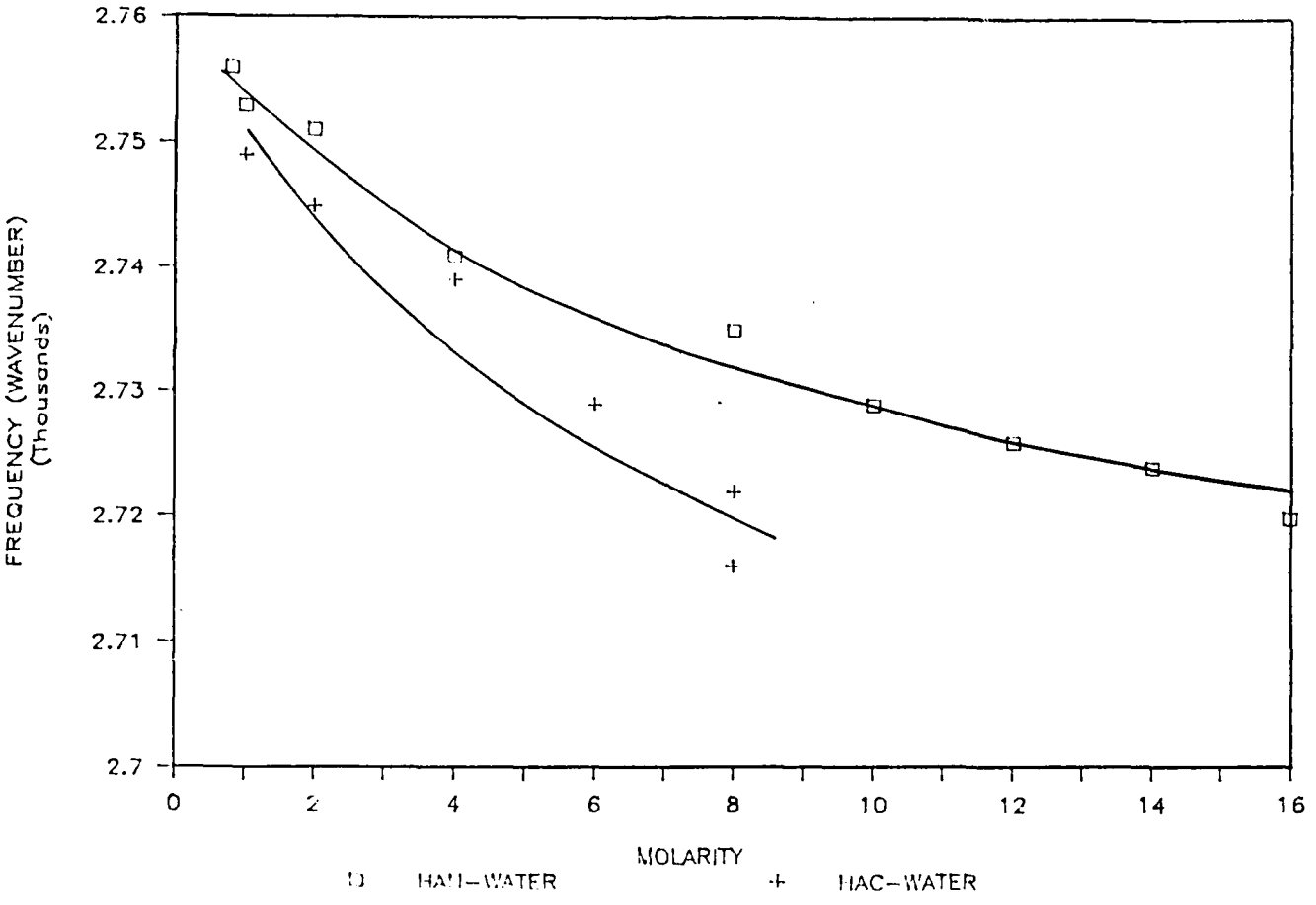

Figure 12. Effect of HA^+ Concentration on the Frequency of the 2720 cm^{-1} Combination Band

Data obtained with HAC solutions are included and, for similar concentrations, maxima are consistently at lower frequencies than are the HAN solutions, indicating that Cl^- interacts more strongly with either the HA^+ or H_2O protons than does NO_3^-.[24] The effect of concentration on the NH_3^+ symmetric stretch near 2955 cm^{-1} are comparable to the combination band (Figure 12) data. Data for the O-H stretch of HAN at about 3150 cm^{-1} are shown in Figure 13.

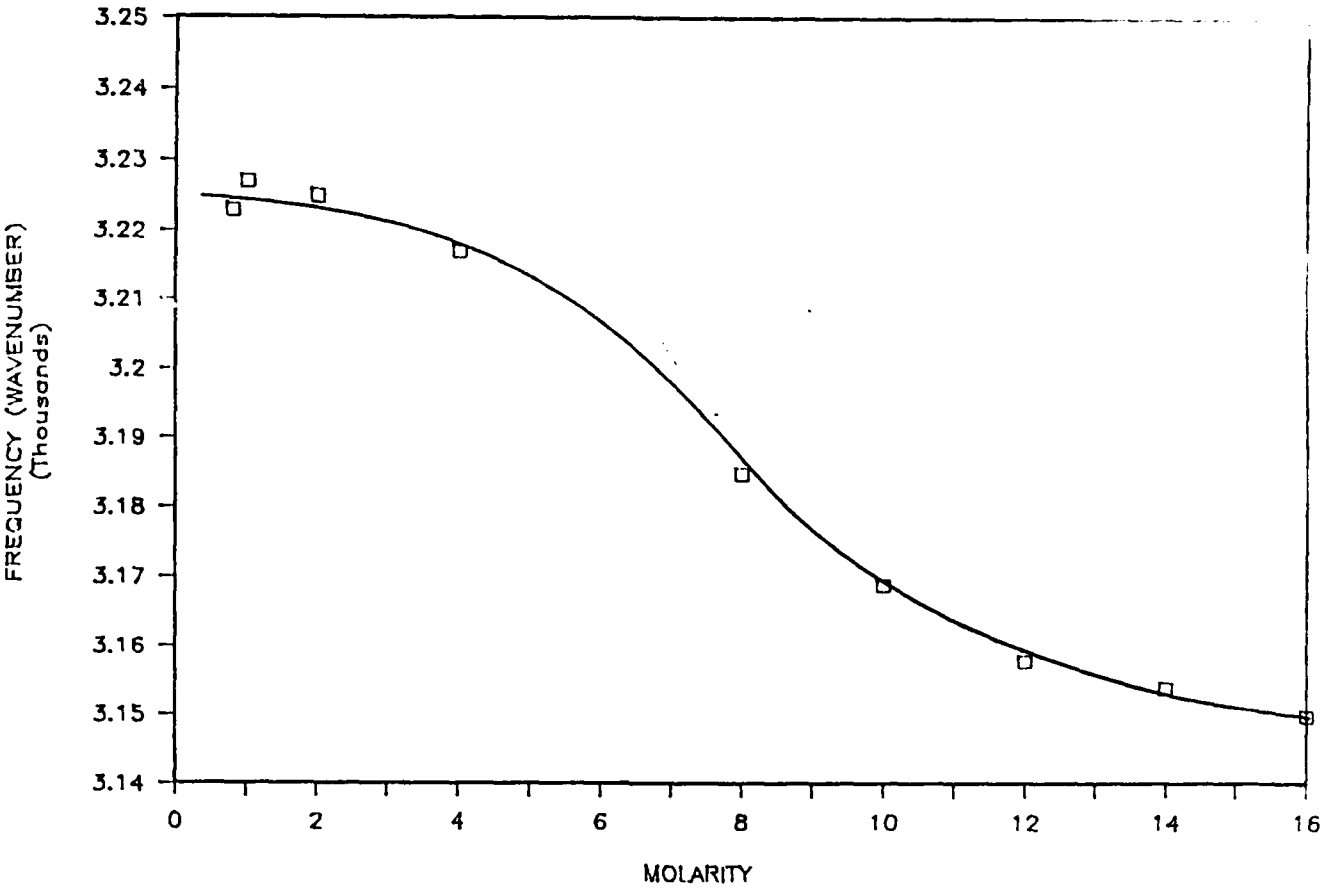

Figure 13. Effect of HAN Concentration on the Frequency of the O-H Stretching Band

One sees that the frequency of the absorbance maximum generally increases with decreasing HAN concentration but that the rate of change is lower at both concentration extremes. The infrared spectra at low HAN concentrations are dominated by a broad water band system, consisting primarily of the asymmetric stretch at about 3400 cm^{-1} and the symmetric stretch at about 3200 cm^{-1}. Quite possibly the data at low HAN concentrations may show interference from the H_2O symmetric stretching band since this band shifts to lower frequency as water concentration increases. There is no indication of interference from water at HAN concentrations above 8 M confirming that the band near 3150 cm^{-1} is indeed due to HAN.

The data of Figure 13 at high HAN concentrations also require comment. Although frequency continues to decrease with increasing salt content, the rate of the decrease slows markedly above 12 M HAN. A possible explanation is that the effect approaches saturation because the interaction causing it is essentially complete, bearing in mind that the 3150 cm^{-1} band should show the effect of ion-pairing via the HA^+ O-H hydrogen.

Since both the N-H and the O-H vibrational frequencies are affected by varying salt concentration, ion-pairing via hydrogen bonding with NO_3^- can and probably does involve both the N-H and O-H hydrogens. The change in O-H frequency as a function of HAN concentration is at least 4 times greater than the change in N-H, indicating that hydrogen bonding via the O-H group is stronger than with N-H. The monotonic increase in vibrational frequency with decreasing HAN concentration indicates that the interaction of HA^+ with water is probably quite weak relative to its interaction with NO_3^- .

The NH_3^+ symmetric deformation near 1512 cm^{-1} and NH_3^+ degenerate rocking near 1179 cm^{-1} are clearly seen in Figure 4. The 1512 cm^{-1} band shifts to lower frequency with increasing HAN concentration and thus further supports the conclusion that interaction of HA^+ with nitrate is stronger than with water. In the case of the 1179 cm^{-1} band, no frequency shift is seen but intensity increases with increasing HAN concentration in much the same manner as is seen in Figure 10. Using an argument parallel to that used in explaining the Figure 10 data, it is concluded that the HA^+ interacts with both water and nitrate and that the interaction with nitrate is stronger than with water.

c. <u>The FTIR spectrum of water</u>. The tetrahydrofuran molecule possesses a dipole moment, so the mutual solubility of water and THF is probably the result of dipole-dipole interaction rather than hydrogen bonding. Thus, hydrogen bonding between water molecules is expected to be the only significant interaction in a water-THF mixture. The spectra (Figure 2) show two distinct features attributable to water, a broad band, the asymmetric stretching mode, appearing in the 3000-3750 cm^{-1} region, and a much narrower band, the O-H bending mode, at 1655 cm^{-1}. Spectral features in the 2780-3010 cm^{-1} region and below 1525 cm^{-1} are due to the THF present in the mixtures.

At higher water concentrations (>20 M) the THF bands at about 2900 cm^{-1} overlap the water bands slightly but can easily be removed by spectral subtraction. The frequency of the absorption maximum in the 3000-3750 cm^{-1} region is concentration dependent, the frequency decreasing as water concentration increases, whereas the frequency of the 1655 cm^{-1} absorption is independent of water concentration.

The change in frequency of the absorption maximum of the asymmetric stretching mode of water as a function of water concentration is shown in Figure 14.

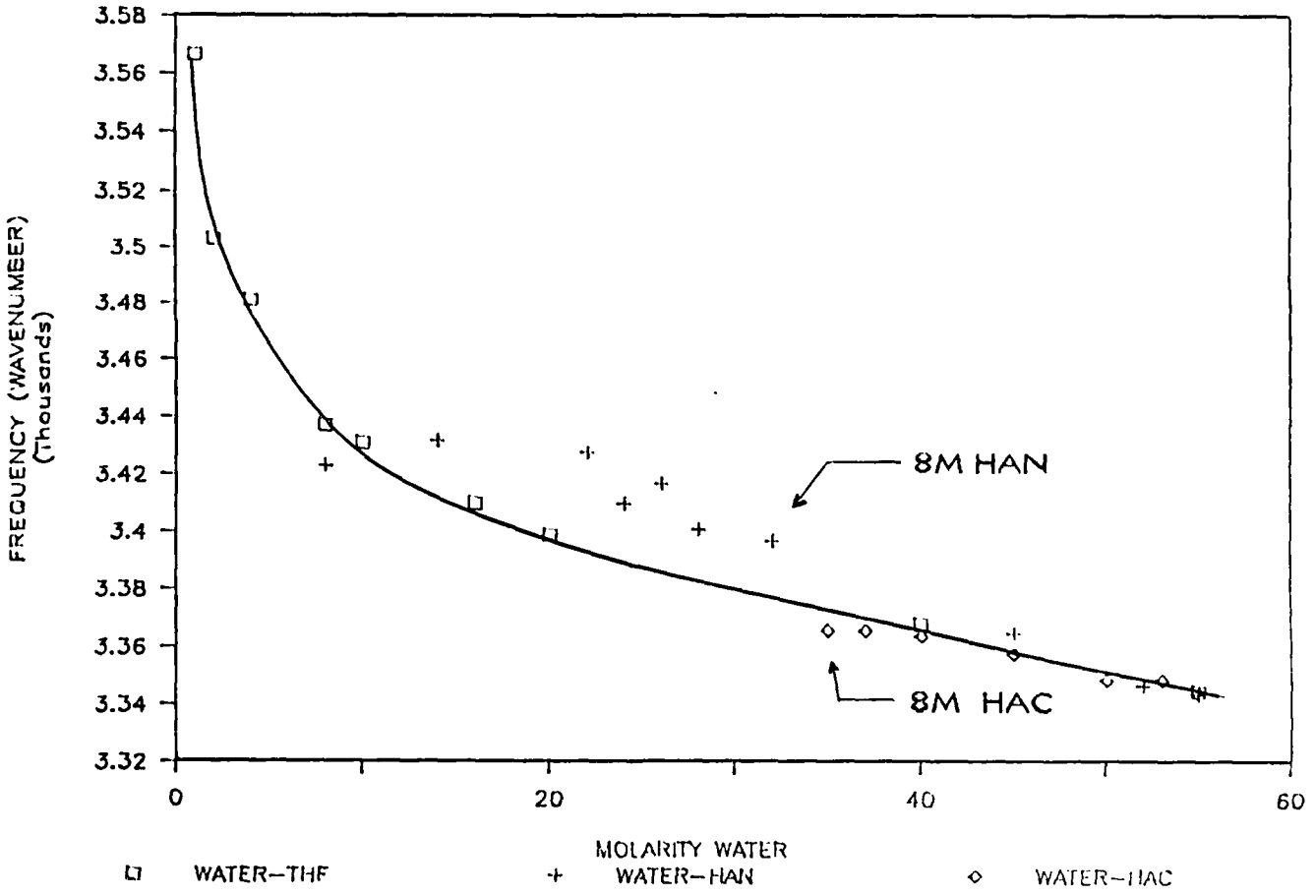

Figure 14. Frequency of the O-H Asymmetric Stretch as a Function of Water Concentration

A smooth curve can be drawn through all of the water-THF points, all of the HAC data, and the HAN data at lower salt concentrations. This indicates that H_2O-H_2O interactions are dominant at low salt concentration. Significant deviation from the curve is seen at HAN concentrations above 4 M where HAN-water interaction appears to disrupt the water structure. The data generally lie above the curve, the higher frequencies indicating that HAN-water interactions are weaker than the interaction of water with itself. The pattern is not well defined although a trend toward an increase in O-H frequency with increasing HAN concentration seems to be present. It is possible that O-H frequency becomes constant above 12 M HAN indicating that the nature of the interaction is quite different in these highly concentrated mixtures from what is seen in the more common aqueous solutions usually studied. In this respect, the data resemble the HA^+ data at high salt content shown in Figure 13. It is possible that a similar explanation, namely that the effect saturates, applies to these data also. Here the basis for saturation of the effect would be that so little water is now present that water-water interactions are essentially reduced to insignificance.

It is unfortunate that HAC saturates in water at room temperature at approximately 8 M because a slight deviation from the water-THF line is seen above 6 M HAC. The points fall below the line indicating that Cl^- interacts more strongly with water than does either nitrate or water itself. The saturation limit prevents pursuit of this matter, although the data support the conclusions reached in the HA^+ spectral investigation regarding the relative strengths of the Cl^--proton and NO_3^--proton interactions.

2. ANALYSIS

An analytical procedure should be direct and unambiguous if possible and should produce a linear response to concen-tration variation over the widest possible range. Many of the vibrational bands discussed above show variations with concentration both in frequency and in intensity. Although such variation permitted evaluation of the structure of the species present in the mixtures, it is most undesirable if FTIR is to be used for sample analysis. The spectra in Figures 2, 3, and 4 contain features that were not discussed previously because their frequency does not change significantly with changing

concentration. These features will now be used as the basis of analytical methods for HAN and water.

a. Analysis of HAN solutions. The water spectra in Figure 2 contain two distinct features, the broad O-H asymmetric stretching band appearing in the 3000-3750 cm^{-1} region, and the much narrower O-H bending band at 1655 cm^{-1}. Although the frequency of the 1655 cm^{-1} absorption is independent of water concentration, inspection of Figure 3 reveals that the band is strongly subject to interference by HAN bands and is thus not available for use in HAN solutions. Frequency of the absorption maximum in the 3000-3750 cm^{-1} region is concentration dependent, the frequency decreasing as water concentration increases. However, integrated peak area varies linearly with water content over the entire concentration range studied, and, as seen in Figure 14, frequency changes rather slowly with concentration over the range 10-30 M. Absorbance at 3420 cm^{-1} is shown as a function of water concentration in Figure 15, ignoring the frequency-concentration dependence entirely.

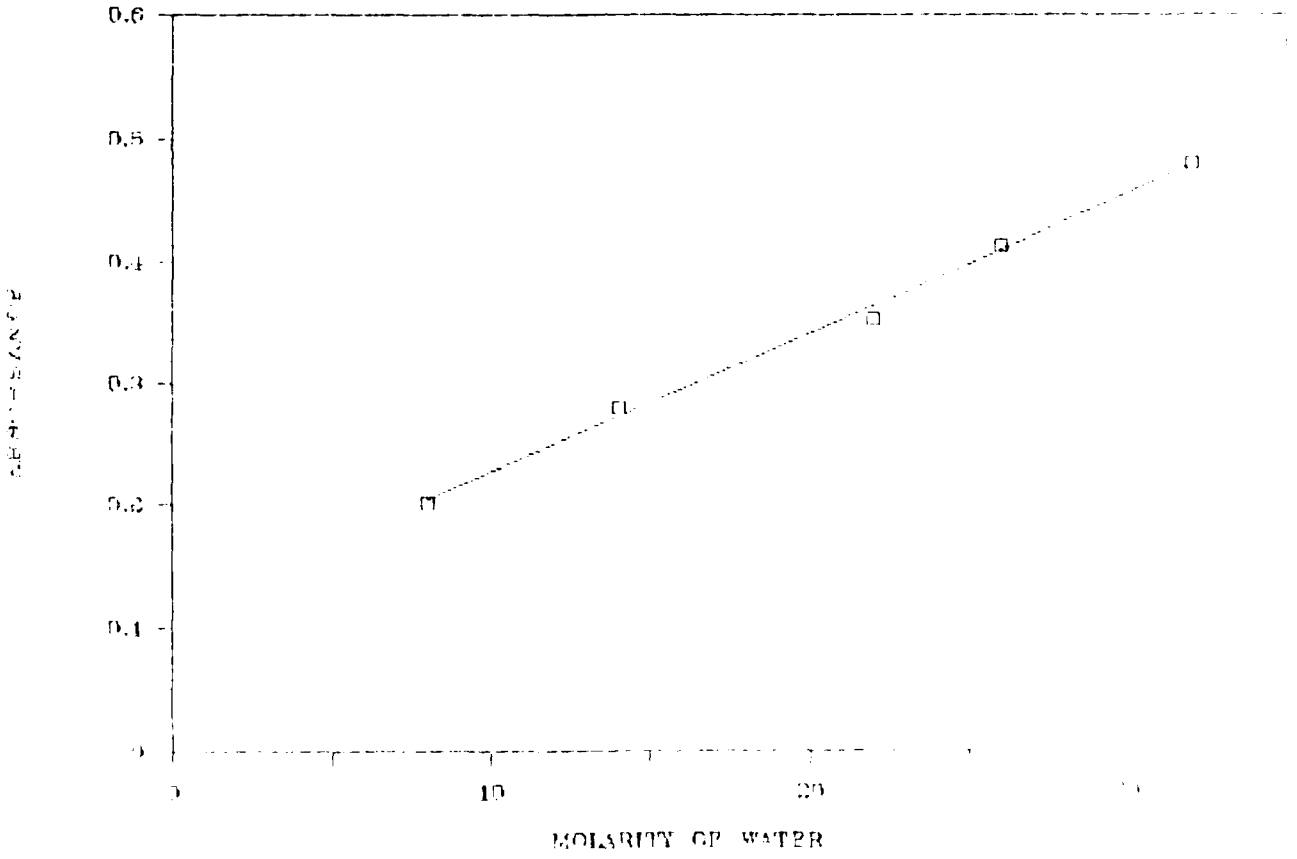

Figure 15. Absorbance at 3420 cm^{-1} as a Function of Water Concentration

The nitrate ion N-O symmetric stretch at 1044 cm^{-1} [19] and the HA^{+} N-O symmetric stretch at 1007 cm^{-1} were not considered in discussing the effect of structure on vibrational spectra because it was felt that these bands would not be responsive to such variation. It is for precisely this reason that the N-O stretching band should be most useful in analytical work. In both cases frequency is not concentration dependent. Linearity of the 1044 cm^{-1} peak is shown in Figure 16 and of the 1007 cm^{-1} peak in Figure 17.

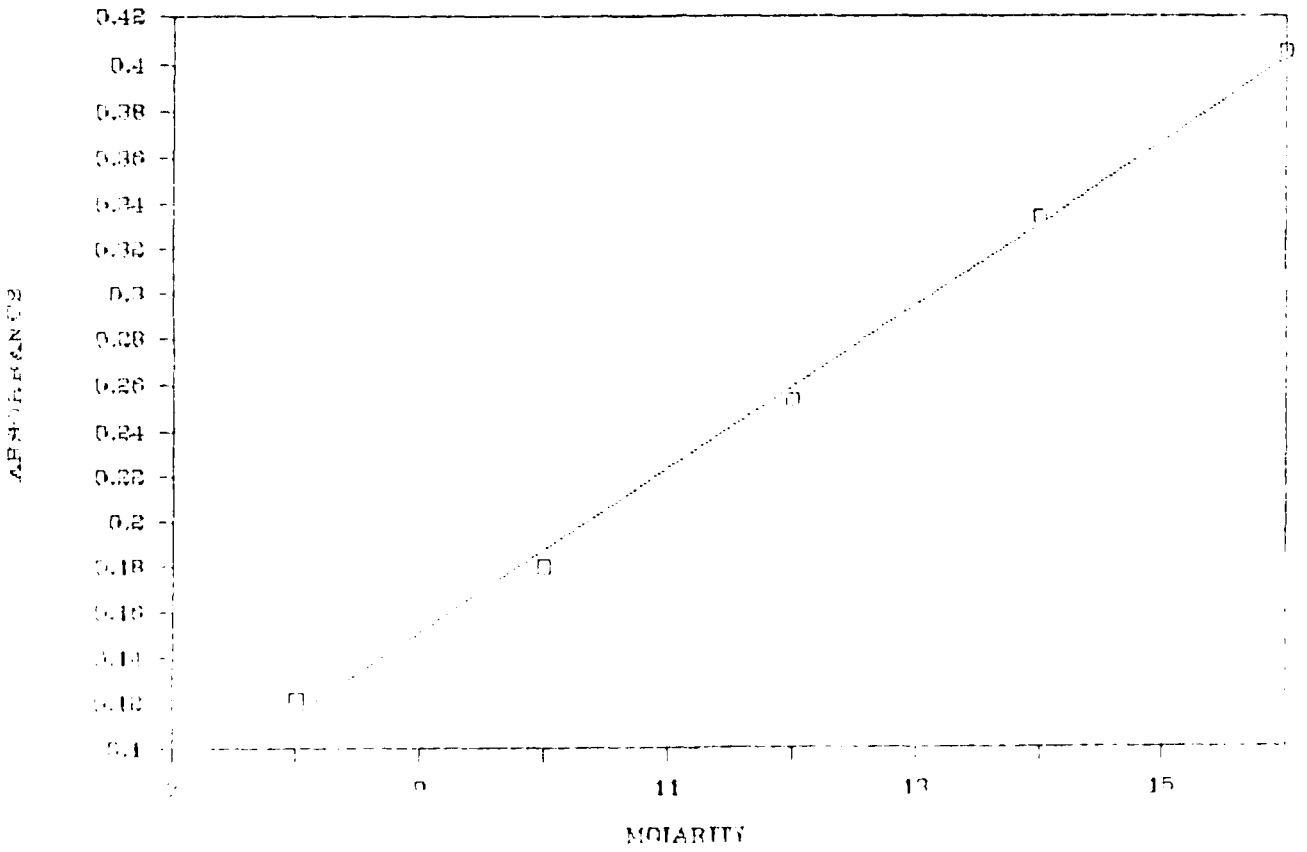

Figure 16. Absorbance at 1044 cm^{-1} as a Function of Nitrate Ion Concentration

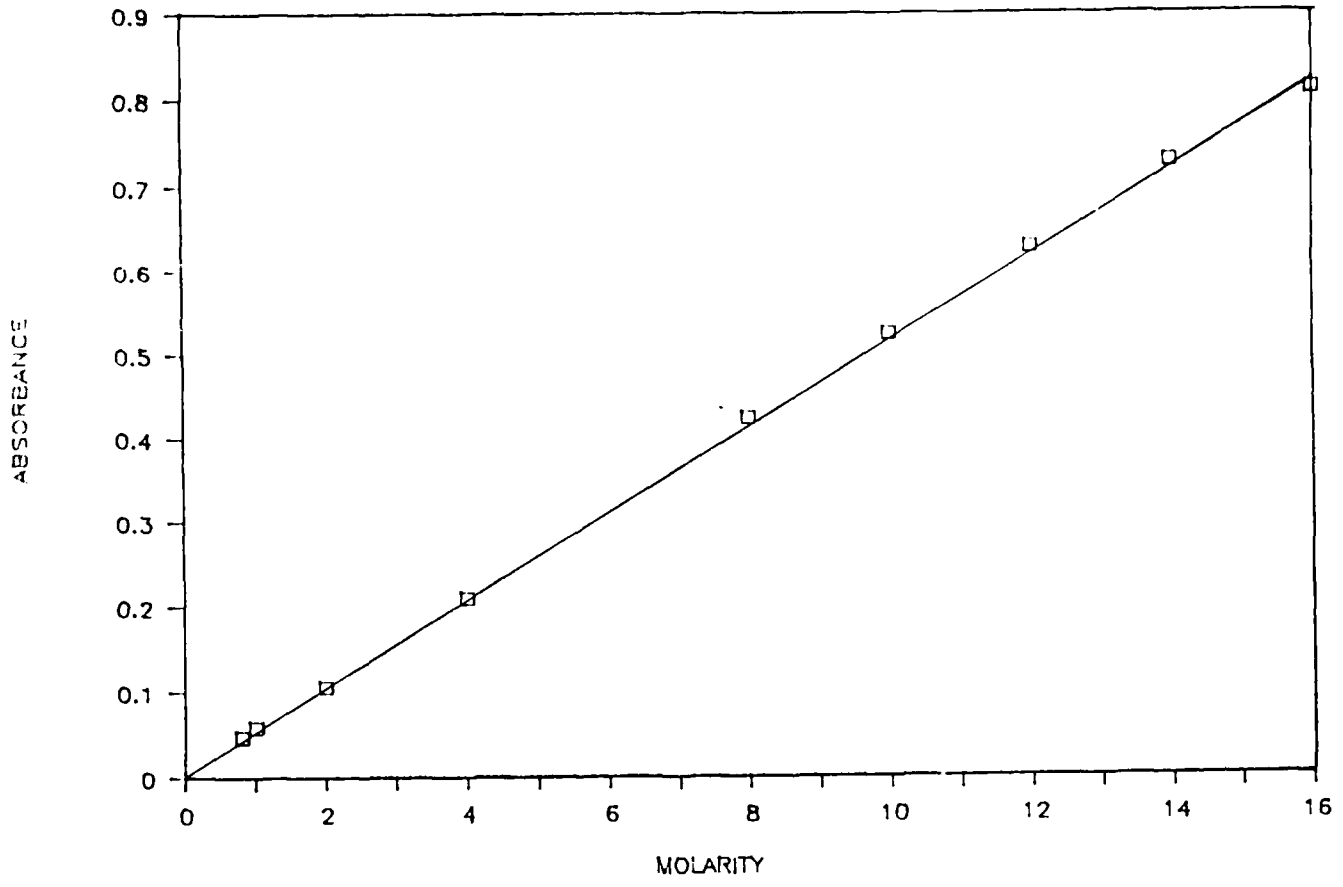

Figure 17. Absorbance at 1007 cm^{-1} as a Function of Hydroxylammonium Ion Concentration

The lines in Figures 15, 16, and 17 were obtained by linear regression of the data. In all cases a correlation coefficient of at least 0.995 is obtained, indicating that absorbance varies linearly with concentration over the concentration range selected.

The HAN emerging from the electrolytic process is approximately 2.5 M and requires concentration to about 14 M to be used in formulating propellant. Over that concentration range, water content varies from 52 to 14 M. The data presented adequately cover the upper HAN and lower water ranges, the regions in which concentration determination and control will be crucial.

Although it is obvious from Figure 4 that the N-O stretching bands are not the most intensely absorbing bands available and, therefore, will not provide the highest analytical sensitivity, they are adequate for the purpose intended. From the slope obtained in Figure 17 (0.0512), a concentration change of 0.09 M in hydroxylammonium ion produces a change of 0.005 in absorbance, a value well within the sensitivity limit of the instrument used. In like manner, the data in Figure 16 indicate a nitrate concentration change of 0.139 M for the same variation in absorbance. If greater concentration sensitivity is required, it can readily be accomplished by increasing the number of discrete reflections within the CIRcle cell. In addition, greater sensitivity can be achieved by an increase in S/N ratio, a procedure that requires co-addition of a larger number of scans, since, within limits, S/N ratio is doubled by quadrupling the number of scans. This is not especially burdensome since a single scan is acquired within a matter of seconds.

The frequency of the O-H asymmetric stretch is concentration dependent but the change is sufficiently small that, as seen in Figure 15, absorbance-concentration linearity at a fixed frequency is retained over a wide concentration range. The slope of the line generated by the Figure 15 data (0.01144) produces an absorbance change of 0.005 for a water concentration change of 0.396 M.

Since the three spectral bands used for sample analysis are acquired from the same scan, errors associated with sample manipulation such as weighings and transfers in serial component analysis are eliminated. Analytical sensitivity, however, is set by the band with the lowest concentration-absorbance variation (the water band). Using the very conservative value of 0.001 change in absorbance as the limit of precision in the analysis, 10 M HAN (26 M water) produces precision limits of $\pm$ 0.34 % for water, $\pm$ 0.20 % for HA^+, and $\pm$ 0.28 % for nitrate. At 14 M HAN (14 M water) these values become $\pm$ 0.63 % for water, $\pm$ 0.20 % for HA^+, and $\pm$ 0.20 % for nitrate. Since 14 M HAN exceeds the HAN concentration needed for propellant formulation and is the water worst case, a precision limit of 0.6 % for the analysis is established.

The use of three bands for sample analysis is doubly [illegible] HAN-water mixture is pure since hydroxylammonium to nitrate ratio must be [illegible] and the sum of HAN and water must equal 100 % of the sample under such conditions. The analytical scheme is therefore quite sensitive to the presence of impurities although no attempt is made to identify them. From the viewpoint of on-line production control, detection of the presence of impurities, rather than determination of their identity or concentration, is the critical matter. In this regard, the analytical scheme outlined is very well suited to the task.

Although the Sirius 100, a research spectrometer, was used to obtain the data presented, simpler instruments utilizing the same optical path are available. These instruments lack many of the features of the research instrument and are therefore not as versatile, nor are they amenable to complex and sophisticated data handling and reduction. They do, however, possess the same optical quality as the research instrument, are simpler to operate, and are probably somewhat more rugged, features that are highly desirable in a production facility. The simpler instruments can also be programmed to use the results of the analysis obtained to control various processes that are an integral part of materiel production such as vacuum level, thermal input, and flow rate. It is anticipated that sampling and analysis will be continuous and that discrete analytical values will be available at intervals of one minute or less. Since the analysis is non-destructive, samples can be returned to the production line eliminating any requirement for waste disposal.

b. Assay of HAN-Based propellants. The propellants LGP 1845 and 1846 contain water, HAN, and TEAN. Although the contents of this report deal mainly with water and HAN, the potential of the FTIR-CIR technique for complete propellant assay should not be overlooked.

The TEAN spectra shown in Figure 5 contain the 1360 cm^{-1} nitrate ion band, seen in Figures 3 and 4 and, as expected, the 1655 cm^{-1} water band is seen. The most obvious differences between the TEAN and HAN spectra are in the 950 - 1100 cm^{-1} region. Although not analysed in detail as yet, we expect that specific bands will be available for analytical use. This expectation

reinforced by the data shown in Figure 6 in which a propellant spectrum synthesized from the spectra of the separate components is compared with the spectrum of LGP 1845. Excellent agreement, both in overall shape and in relative peak height, is observed although detailed investigation of the TEAN-water and TEAN-HAN-water interactions are required before such analyses can be proposed with the degree of certainty presently available for the HAN-water system.

V. CONCLUSIONS

The infrared spectrum of the nitrate ion in aqueous HAN indicates that ion-pairs are formed in these solutions. Evidence for cation-anion contact is seen at relatively low salt concentration although hydration of the nitrate ion is seen and is still dominant. Hydration is readily observed as a splitting of the degenerate ν_3 mode at HAN concentrations as low as 0.01 M, concentrations in which ion-pairing is probably unimportant. As HAN concentration increases, a strongly hydrogen-bonded, cation-anion pair becomes the major species, interactions being much stronger than those of the ions with solvent. The ion-pairs become the dominant species at about 8 M. All of the nitrate data support the existence of two nitrate species in these mixtures although the ν_3 data are the least equivocal. The data are self-consistent showing the formation of a nitrate species at low salt concentration that is gradually converted to a second species as salt content increases.

The infrared spectrum of the hydroxylammonium ion supports these conclusions and provides evidence concerning the nature of the hydrogen bonds formed. The HA^+ ion has C_s symmetry[12] with the O-H hydrogen and one of the N-H hydrogens lying in the C_s plane. The nitrate ion can interact with any of the hydrogens, producing three ion-pair orientations. Although the specific ion-pairs are not resolved in the FTIR spectrum, there is evidence that the O-H proton is the preferable site for hydrogen bonding. In this regard, the structure of the ion-pair strongly resembles the structure obtained by crystallographic analysis of solid HAN.[30]

Ion hydration is also observed as a perturbation of the water spectrum at low salt concentrations. With increasing salt content, water structure is disrupted, indicated by a significant increase in the O-H stretch frequency. In this context HAN can be considered a structure breaker, $H_2O\text{-}NO_3^-$ and $H_2O\text{-}HA^+$ bonding being stronger than $H_2O\text{-}H_2O$ bonding.

An analytical scheme, based on the FTIR spectrum of HAN, has been developed. The scheme is doubly redundant and is, therefore, highly sensitive to the presence of impurities. The scheme is accurate, is capable of analysis with a precision of $\pm$ 0.6 %, and seems well suited for use in a manufacturing facility to provide on-line analysis and process control. Although not addressed herein, it is expected that the equipment and technique used will be equally capable of analysing and controlling TEAN production, the third component in LGP 1845 and LGP 1846.

The use of FTIR spectroscopy for propellant assay has a number of virtues, not the least of which is simultaneous analysis of all of the major components of the mixture. Although the equipment required is fairly expensive and requires training and expertise for proper operation and maintenance, experience has been that the system is sufficiently stable to permit unattended operation for extended periods. On-line monitoring and control of the concentration and purity of propellant components are obvious applications of this analytical method, which makes the technique especially well suited for production quality control and product assurance. Automated and rapid analysis of large numbers of samples obviates the initial high cost of the equipment, which, with appropriate programming, can be used to control the entire component production and propellant blending process. The spectral richness, in general, of high-resolution FTIR spectra permits detection of contaminants although their identification and quantitative determination is a far more complex matter. For purposes of quality control, however, detection is often all that is required.

REFERENCES

1. Sasse, R.A. and Klein, N., "Thermal Initiation of Hydroxylammonium Nitrate Based Gun Propellants," Proc. 15th JANNAF Combustion Meeting, Vol I, p 313, CPIA Pub. 297, Chemical Propulsion Information Agency, Laurel, MD, 1979.

2. Klein, N., "Preparation and Characterization of Several Liquid Propellants," Rept. ARBRL-TR-02471, U.S. Army Ballistic Research Laboratory, Aberdeen Proving Ground, MD, 1983.

3. Klein, N., Decker, M.M., Leveritt, C.S., and Wojciechowski, J.Q., "Low Temperature Calorimetry of HAN-Based Propellants," Proc. 23rd JANNAF Combustion Meeting, Vol III, p 133, CPIA Pub. 457, Chemical Propulsion Information Agency, Laurel, MD, 1986.

4. Decker, M.M., Freedman, E., Klein, N., Leveritt, C.S., and Wojciechowski, J.Q., "Liquid Propellant Physical Properties," BRL-TR-in press, US Army Ballistic Research Laboratories, Aberdeen Proving Ground, MD.

5. Griffiths, P.R., "Chemical Infrared Fourier Transform Spectroscopy," Wiley-Interscience, New York, 1975.

6. Harrick, N.J., "Internal Reflection Spectroscopy," Wiley-Interscience, New York, 1967.

7. Bertie, J.E. and Eysel, H.H., Appl. Spectrosc. Vol. 39, p 392, (1985).

8. Dotson, R.L., "High Purity HAN Study," Final Report, Contract DAAK15-85-C-0001, Olin Corp., New Haven, CT, 1986.

9. Biddle, R.A., private communication.

10. Fifer, R.A. and Cronin, J.T., "Determination of Liquid Propellant Composition by a Fourier Transform Infrared-Cylindrical Internal Reflection (FTIR-CIR) Technique," Proc. 1984 JANNAF Propellant Characterization Subcommittee Meeting, CPIA Pub. 413, p 205, Chemical Propulsion Information Agency, Laurel, MD, 1985.

11. Decker, M.M., Klein, N., and Wong, K.N., Proc. 17th Int. ICT Symp, p 61, 1986.

12. Frasco, D.L. and Wagner, E.L., J. Chem. Phys. 30, 1124 (1959).

13. Rocchiccioli, C., Compt. Rendu. Acad. Sci. 253, 838 (1961).

14. Van Dijk, C.A. and Priest, R.G., Combustion and Flame, 57, 15 (1984).

15. Cronin, J.T. and Brill, T.B., J. Phys. Chem. 90, 178 (1986).

16. Fifer, R.A., "Application of Isotopic Uncoupling Vibrational Spectroscopy to Structural Determination for HAN-Based Liquid Propellants," Proceedings 21st JANNAF Combustion Meeting, Vol II, p 529, CPIA Pub. 412, Vol 2, p 529, 1984, Chemical Propulsion Information Agency, Laurel, MD, 1984.

17. Novak, A., "Hydrogen Bonding in Solids. Correlation of Spectroscopic and Crystallographic Data," Structure and Bonding, Vol. 18, Springer-Verlag, NY, 1974.

18. Vanderhoff, J.A. and Bunte, S.W., "Laser Raman Studies Related to Liquid Propellants: Structural Characteristics," Proceedings 22nd JANNAF Combustion Meeting, Vol II, p 187, CPIA Pub. 432, Chemical Propulsion Information Agency, Laurel, MD, 1985.

19. Irish, D.E. and Brooker, M.H., "Raman and Infrared Spectral Studies of Electrolytes," Chap. 6 in "Advance In Infrared And Raman Spectroscopy," Vol. 2, R.J.H. Clark and R.E. Hester, Ed., Heyden & Son Ltd., NY, 1976.

20. Janz, G.J. and Kozlowski, T.R., J. Chem. Phys., 40, 1699 (1964).

21. Hester, R.E. and Plane, R.A., J. Chem. Phys. 40, 411 (1964).

22. Irish, D.E. and Davis, A.R., Can. J. Chem. 46, 943 (1968).

23. Davis, A.R. and Plane, R.A., J. Chem. Phys. 50, 2262 (1969).

24. Davis, A.R., Macklin, J.W., and Plane, R.A., J. Chem. Phys. 50, 1478 (1969).

25. Findlay, T.J.V. and Symons, M.C.R., J. Chem. Soc., Faraday Trans.II, 72, 820 (1976).

26. Nelson, D.L. and Irish, D.E., J. Chem. Phys. 54, 4479 (1971).

27. Riddell, J.D., Lockwood, D.J., and Irish, D.E., Can. J. Chem. 50, 2951 (1972).

28. Bunte, S.W., Vanderhoff, J.A., and Donmoyer, P.M., "Electrical Conductivity Measurements on Hydroxylammonium Nitrate," Proceedings 22nd JANNAF Combustion Meeting, Vol II, p 195, CPIA Pub. 432, Chemical Propulsion Information Agency, Laurel, MD, 1985.

29. Plowman, K.R. and Lagowski, J.J., J. Phys. Chem. 78, 143 (1974).

30. Rheingold, A.L., Cronin, J.T., Brill, T.B. and Ross, F.K., Acta Crystall.-in press.

DISTRIBUTION LIST

No. of Copies	Organization
12	Commander Defense Technical Info Center ATTN: DTIC-DDA Cameron Station Alexandria, VA 22304-6145
1	Director Defense Advanced Research Projects Agency ATTN: H. Fair 1400 Wilson Boulevard Arlington, VA 22209
1	HQDA DAMA-ART-M Washington, DC 20310
1	Commander US Army Materiel Command ATTN: AMCDRA-ST 5001 Eisenhower Avenue Alexandria, VA 22333-0001
13	Commander Armament R&D Center US Army AMCCOM ATTN: SMCAR-TSS SMCAR-TDC SMCAR-SCA, B. Brodman R. Yalamanchili SMCAR-AEE-B, D. Downs A. Beardell SMCAR-LCE, N. Slagg SMCAR-LCS, W. Quine A. Bracuti J. Lannon SMCAR-FSS-A, R. Price L. Frauen SMCAR-FSA-S, H. Liberman Picatinny Arsenal, NJ 07806-5000
3	Director Benet Weapons Laboratory Armament R&D Center US Army AMCCOM ATTN: SMCAR-LCB-TL E. Conroy A. Graham Watervliet, NY 12189
1	Commander US Army Armament, Munitions and Chemical Command ATTN: SMCAR-ESP-L Rock Island, IL 61299-7300
1	Commander US Army Aviation Research and Development Command ATTN: AMSAV-E 4300 Goodfellow Blvd. St. Louis, MO 63120
1	Commander Materials Technology Lab US Army Laboratory Cmd ATTN: SLCMT-MCM-SB M. Levy Watertown, MA 02172-0001
1	Director US Army Air Mobility Rsch. and Development Lab. Ames Research Center Moffett Field, CA 94035
1	Commander US Army Communications Electronics Command ATTN: AMSEL-ED Fort Monmouth, NJ 07703
1	Commander ERADCOM Technical Library ATTN: STET-L Ft. Monmouth, NJ 07703-5301

DISTRIBUTION LIST

No. of Copies	Organization
1	Commander US Army Harry Diamond Labs ATTN: DELHD-TA-L 2800 Powder Mill Rd Adelphi, MD 20783
1	Commander US Army Missile Command Rsch, Dev, & Engr Ctr ATTN: AMSMI-RD Redstone Arsenal, AL 35898
1	Commander US Army Missile & Space Intelligence Center ATTN: AIAMS-YDL Redstone Arsenal, AL 35898-5500
1	Commander US Army Belvoir R&D Ctr ATTN: STRBE-WC Tech Library (Vault) B-315 Fort Belvoir, VA 22060-5606
1	Commander US Army Tank Automotive Cmd ATTN: AMSTA-TSL Warren, MI 48397-5000
1	Commander US Army Research Office ATTN: Tech Library P.O. Box 12211 Research Triangle Park,NC 27709-2211
1	Director US Army TRADOC Systems Analysis Activity ATTN: ATAA-SL White Sands Missile Range NM 88002
1	Commandant US Army Infantry School ATTN: ATSH-CD-CSO-OR Fort Benning, GA 31905
1	Commander Armament Rsch & Dev Ctr US Army Armament, Munitions and Chemical Command ATTN: SMCAR-CCS-C, T Hung Picatinny Arsenal, NJ 07806-5000
1	Commandant US Army Field Artillery School ATTN: ATSF-CMW Ft Sill, OK 73503
1	Commandant US Army Armor Center ATTN: ATSB-CD-MLD Ft Knox, KY 40121
1	Commander US Army Development and Employment Agency ATTN: MODE-TED-SAB Fort Lewis, WA 98433
1	Commander Naval Surface Weapons Center ATTN: D.A. Wilson, Code G31 Dahlgren, VA 22448-5000
1	Commander Naval Surface Weapons Center ATTN: Code G33, J. East Dahlgren, VA 22448-5000
2	Commander US Naval Surface Weapons Ctr. ATTN: O. Dengel K. Thorsted Silver Spring, MD 20902-5000
1	Commander Naval Weapons Center China Lake, CA 93555-6001
1	Commander Naval Ordnance Station ATTN: C. Dale Code 5251 Indian Head, MD 20640

DISTRIBUTION LIST

No. of Copies	Organization
1	Superintendent Naval Postgraduate School Dept of Mechanical Eng. ATTN: Code 1424, Library Monterey, CA 93943
1	AFWL/SUL Kirtland AFB, NW 87117
1	Air Force Armament Lab ATTN: AFATL/DLODL Eglin, AFB, FL 32542-5000
1	AFOSR/NA (L. Caveny) Bldg. 410 Bolling AFB, DC 20332
1	Commandant USAFAS ATTN: ATSF-TSM-CN Ft Sill, OK 73503-5600
1	US Bureau of Mines ATTN: R.A. Watson 4800 Forbes Street Pittsburgh, PA 15213
1	Director Jet Propulsion Lab ATTN: Tech Libr 4800 Oak Grove Drive Pasadena, CA 91109
2	Director National Aeronautics and Space Administration ATTN: MS-603, Tech Lib MS-86, Dr. Povinelli 21000 Brookpark Road Lewis Research Center Cleveland, OH 44135
1	Director National Aeronautics and Space Administration Manned Spacecraft Center Houston, TX 77058
10	Central Intelligence Agency Office of Central Reference Dissemination Branch Room GE-47 HQS Washington, DC 20502
1	Central Intelligence Agency ATTN: Joseph E. Backofen HQ Room 5F22 Washington, DC 20505
4	Bell Aerospace Textron ATTN: F. Boorady K. Berman A.J. Friona J. Rockenfeller Post Office Box One Buffalo, NY 14240
1	Calspan Corporation ATTN: Tech Library P.O. Box 400 Buffalo, NY 14225
7	General Electric Ord. Sys Dpt ATTN: J. Mandzy, OP43-220 R.E. Mayer H. West M. Bulman R. Pate I. Magoon J. Scudiere 100 Plastics Avenue Pittsfield, MA 01201-3698
1	General Electric Company Armanent Systems Department ATTN: D. Maher Burlington, VT 05401
1	IITRI ATTN: Library 10 W. 35th St. Chicago, IL 60616
1	Olin Chemicals Research ATTN: David Gavin P.O. Box 586 Chesire, CT 06410-0586

DISTRIBUTION LIST

No. of Copies	Organization
2	Olin Corporation ATTN: Victor A. Corso Dr. Ronald L. Dotson P.O. Box 30-9644 New Haven, CT 06536
1	Paul Gough Associates ATTN: Paul Gough PO Box 1614 Portsmouth, NH 03801
1	Safety Consulting Engr ATTN: Mr. C. James Dahn 5240 Pearl St. Rosemont, IL 60018
1	Science Applications, Inc. ATTN: R. Edelman 23146 Cumorah Crest Woodland Hills, CA 91364
1	Sunstrand Aviation Operations ATTN: Dr. Owen Briles P.O. Box 7002 Rockford, IL 61125
1	Veritay Technology, Inc. ATTN: E. B. Fisher 4845 Millersport Highway, P.O. Box 305 East Amherst, NY 14051-0305
1	Director Applied Physics Laboratory The Johns Hopkins Univ. Johns Hopkins Road Laurel, Md 20707
2	Director Chemical Propulsion Info Agency The Johns Hopkins Univ. ATTN: T. Christian Tech Lib Johns Hopkins Road Laurel, MD 20707
2	University of Delaware Department of Chemistry ATTN: Mr. James Cronin Professor Thomas Brill Newark, DE 19711
1	U. of ILLinois at Chicago ATTN: Professor Sohail Murad Dept of Chemical Eng Box 4348 Chicago, IL 60680
1	U. of Maryland at College Park ATTN: Professor Franz Kaspar Department of Chemistry College Park, MD 20742
1	U. of Missouri at Columbia ATTN: Professor R. Thompson Department of Chemistry Columbia, MO 65211
1	U. of Michigan ATTN: Prof. Gerard M. Faeth Department of Aerospace Engineering Ann Arbor, MI 48109-3796
1	U. of Missouri at Columbia ATTN: Professor F. K. Ross Research Reactor Columbia, MO 65211
1	U. of Missouri at Kansas City Department of Physics ATTN: Prof. R.D. Murphy 1110 East 48th Street Kansas City, MO 64110-2499
1	Pennsylvania State University Dept. of Mechnical Eng ATTN: K. Kuo University Park, PA 16802

DISTRIBUTION LIST

No. of Copies	Organization
2	Princeton Combustion Rsch Laboratories, Inc. ATTN: N.A. Messina M. Summerfield 475 US Highway One North Monmouth Junction, NJ 08852
1	University of Arkansas Department of Chemical Engineering ATTN: J. Havens 227 Engineering Building Fayetteville, AR 72701

Aberdeen Proving Ground

Dir, USAMSAA
ATTN: AMXSY-D
AMXSY-MP, H. Cohen

Cdr, USATECOM
ATTN: AMSTE-TO-F

CDR, CRDEC, AMCCOM
ATTN: SMCCR-RSP-A
SMCCR-MU
SMCCR-SPS-IL

USER EVALUATION SHEET/CHANGE OF ADDRESS

This Laboratory undertakes a continuing effort to improve the quality of the reports it publishes. Your comments/answers to the items/questions below will aid us in our efforts.

1. BRL Report Number_____ Date of Report_____

2. Date Report Received_____

3. Does this report satisfy a need? (Comment on purpose, related project, or other area of interest for which the report will be used.)_____

4. How specifically, is the report being used? (Information source, design data, procedure, source of ideas, etc.)_____

5. Has the information in this report led to any quantitative savings as far as man-hours or dollars saved, operating costs avoided or efficiencies achieved, etc? If so, please elaborate._____

6. *General Comments.* What do you think should be changed to improve future reports? (Indicate changes to organization, technical content, format, etc.)

CURRENT ADDRESS

Name

Organization

Address

City, State, Zip

7. If indicating a Change of Address or Address Correction, please provide the New or Correct Address in Block 6 above and the Old or Incorrect address below.

OLD ADDRESS

Name

Organization

Address

City, State, Zip

(Remove this sheet, fold as indicated, staple or tape closed, and mail.)